

Author response to the referee comments to the paper by Sofiev et al:

Multi-model ensemble simulations of olive pollen distribution in Europe in 2014

First of all, we would like to thank both reviewers for their efforts and comments, which helped us improving the paper. Below, we address them one by one (the comments themselves are included in *italic*).

A general remark.

We would like to emphasize that this is the first-ever experiment of numerical modelling of the European-scale olive pollen dispersion. It was stated in the introduction of the original paper and stressed more in the revised paper, starting from the slightly modified title. Therefore, revealing the issues with the models performance and reporting them to the scientific community was one of the goals of the paper. The issues are reported upfront, were discussed already in the initial paper and addressed in more details in the revised manuscript. In particular, we added a new section 5.4, which summarizes the challenges.

Responses to individual comments of the referees

Referee 1, Slawomir Potempsky

The ensemble setup is based on 6 models, 5 of them using the same meteorological data (ECMWF IFS). This means that this ensemble concerns, in principle, dispersion models – meteorological variety is practically disregarded. From statistics point of view such number of the models can be not enough in real application, but can be treated as a first step. It seems that adding models driven by different meteo data could be important in case of building operational system of this type modelling.

We agree that the current ensemble is at the lower edge of reasonable sizes of such ensembles. Within CAMS, work is going on to increase the number of models up to 10. Possibility to expand the ensemble using perturbed-meteorology forecasts certainly deserves consideration. A sentence stressing the same-meteo-same-source limitation was added in section 5.2.1 and the summary.

29 *The authors proposed also an “optimized ensemble” model basing on properly chosen linear*
30 *combination. This model has shown good skills although the choice of some parameters (like alpha,*
31 *beta) seems to be rather art than to be based on pure mathematical approach.*

32 We have tested several levels for the regularization strength and the selected values have come out
33 of these tests. The limited size of the datasets and short duration of the season constrained the
34 possibilities for data-driven selection of the regularization strength.

35

36 *The presented results have shown some capabilities of the constructed ensemble but also indicated*
37 *problems like the shift of the whole season. This needs further research and is strictly related to*
38 *meteorological forecast.*

39 We agree, the corresponding sentences are included in section 5.2.1 and newly created sub-section
40 5.4. Future challenges

41

42 *1. Paragraph at lines 186-197*

43 *This paragraph needs to be revised in order to precisely define the quantities in the formulas (1)*
44 *and (2) . In the first formula the meaning of t is ambiguous: $a_m(t)$ means coefficients depending on*
45 *the interval t while $c_m(\dots, t)$ means concentration at time t . I think it's better to use parameter*
46 *“tau” for the period (as in the second formula) and t for time point. Thus c_{opt} should depend on*
47 *both tau and t and in the second formula A should depend on tau. There are no definitions of a_0*
48 *(bias depending on ?) in formula (1) and c_0 (observations I guess) in formula (2). Functional J*
49 *should be rather a function of time t than the period tau (unless the average over time is considered*
50 *– but even then the average period time can differ from the period tau used for the analysis).*

51 Corrected

52

53 *2. Definition of SPI – Seasonal Pollen Index – is this follows the description given at the beginning*
54 *of section 3.3 ? It would be good to know whether this index is related to exceeding some threshold*
55 *limit used for allergy risk.*

56 Clarification is added in sections 3.3. What concerns the relation to the allergy-relevant threshold,
57 unfortunately, there is no unified value for it. Extensive discussions have this-far led to conclusion
58 that it is person-specific and chances for generalization are thin. More than that, experience of

59 HIALINE project showed a large variability of the amount of allergen content in the pollen grains,
60 which creates further problems in automatic projection of the pollen forecasts to allergy. References
61 are added to introduction and section 4.1.

62

63 *3. Relating to the previous comments what seems important is to show the agreement of the model*
64 *predictions with the observations basing on the exceedance of threshold limit (as used, for example,*
65 *in allergy forecast). Fig. 4 shows hourly olive pollen concentration – this picture could be*
66 *accompanied by the other presenting agreement on threshold level with the observation.*

67 Unfortunately, as it follows from the above, such threshold does not exist. We have calculated
68 parameters, such as odds ratio etc, in previous papers for birch but the thresholds were each time
69 picked as “expert guess” and criticized in follow-up discussions. Therefore, for the current paper,
70 we concentrated on quality of representation of the season propagation.

71

72 *4. As accumulation heat is one of the crucial parameter the question arises whether it can be*
73 *somehow taken from observations and data assimilation technique can be applied to include such*
74 *information into ensemble modelling.*

75 Temperature is among the most-heavily assimilated meteorological parameters, so bringing it here
76 once again looks like a double-counting. The problem definitely exists but may have more
77 dimensions. In the revised paper, we stressed that it is the combination of the heat-sum
78 accumulation procedure, the flowering threshold, and characteristics of meteorological data that
79 comprise the quality of the season forecast.

80

81 *5. A delicate matter is the calculation of the source term. Thus the question arises whether*
82 *uncertainty of the source term could be a part of modelling i.e. the whether the models' simulation*
83 *could be also performed with perturbations of source term. This, with no doubts, would be time*
84 *consuming, nevertheless having an ensemble system with such capability would be an added value.*
85 *This can be one of the possibility of further development of the system.*

86 We agree. The possibility of perturbing also the source term characteristics is now mentioned in the
87 discussion.

88

89 *Technical remarks*

90 *1. Quality of some figures could be improved:*

91 *a) On Fig. 3 observation points are not well visible – some example locations could be shown on*
92 *separate graph – for example the ones with high values.*

93 *b) Zooming maps on Figs 5 and 6 can improve quality.*

94 *c) parts of Figs 10 and 11 are not well visible.*

95 The figure 3 has been split to two and zooming sub-picture added. The maps were zoomed-in, their
96 color coding improved for better visibility. Figures 10 and 11 are made with high resolution, which
97 allows their zoom at the screen.

98

99 **Anonymous Referee 3**

100 *2. The paper presents an existing concept – the MACC pollen dispersion modelling ensemble*
101 *published by Sofiev et al (2015). As such the idea and the concept has already been published. The*
102 *ensemble is applied on a new pollen type.*

103 Not quite. This paper, indeed building on the existing CAMS ensemble principles, also significantly
104 develops them in several directions. First of all, this is the first numerical simulations for olives
105 made at European level. Secondly, we expanded the ensemble technology of CAMS by
106 constructing the first-ever fusion model for pollen forecasts – and demonstrated its superiority over
107 the simpler ensemble techniques. These main steps forwards are highlighted in the revised paper.

108

109 *The model manuscript use observations, but there is no station list and no accurate numerical or*
110 *accurate description of observations.*

111 We have created the full list of stations and reported the basic statistical metrics for all models. Due
112 to its size, the table is put into supplementary material.

113

114 *3. There are substantial conclusions in the manuscript. However these conclusions do not appear to*
115 *be founded with data presented in the study. One example is the systematic bias in surface*
116 *temperatures as a cause of model uncertainties. However the manuscript does not contain data*
117 *(Figures or tables) concerning surface temperatures.*

118 There seems to be a misunderstanding: our conclusions do not have any sentence regarding the
119 temperature bias of the IFS meteo model. The only reverberation on the quality of this parameter
120 refers to section 5.1 (second paragraph) but that one discussed WRF rather than the core meteo data
121 of IFS. We removed that sentence and reformulated the one in the first paragraph to avoid
122 confusion and to stress that the problem originates from the inconsistency between the features of
123 the temperature forecasts and way they are treated by the source term.

124

125 *Another example is the conclusion that the model calculations represent large scale transport fairly*
126 *well. However the results do not seem to agree with previous observations of olive pollen in Europe*
127 *(Sofiev and Bergmann, 2013). This conclusion there needs better support in the manuscript. The*
128 *maps in figure 3 show that both the ensemble mean and ensemble median calculates a relevant*
129 *seasonal pollen index in Northern France, UK, Germany, Poland. For individual models this is*
130 *extended even to Norway. To my knowledge, olive pollen are rarely or have never been reported*
131 *from those regions. This shows that the ensemble overestimate the large scale atmospheric*
132 *transport. The authors clearly write that the sources in France, presented in the source map, are*
133 *unrealistic low. Adding the missing sources in France must be expected to increase the calculated*
134 *pollen index in nearby regions such as Germany, UK, Poland, Netherlands etc even more. How*
135 *much is naturally not known. Nevertheless, the arguments described above, disagrees with the*
136 *conclusion that the ensemble represent large scale transport fairly well by using the available*
137 *material in the manuscript.*

138 This is indeed a very relevant discussion and the revised paper has more support for the claim. In
139 particular, we expanded the list of stations including Israel (with own olive plantations but remote
140 from major sources in Western Mediterranean). We also refer to Hungarian observations and the
141 corresponding SILAM predictions, albeit made for 2016. Since Hungary has no olive plantations,
142 all pollen there is long-range – and the main episodes were predicted by the model.

143 Also, one limitation has to be kept in mind: The SPI below several tens of pollen day m^{-3} is
144 generally irrelevant from allergy point of view and is very inaccurately observed. The Hirst trap is
145 unreliable up to concentrations as high as 5-10 pollen m^{-3} – such days should be disregarded (Buters
146 et al., 2015, 2012; Galan et al., 2013). In Central- and Northern-European countries, olive pollens
147 are not counted / reported due to their low contribution to the allergy level, high uncertainty and
148 noticeable costs of inflating the list of reported pollens. Therefore, we could not use their data and
149 the evaluation of the transport events inevitably relied on the same network of stations as for the
150 main season. However, looking at northern Spain, it is seen (just qualitatively) that the decrease of

151 modelled total load is as fast as or even faster than that in the observations. Since the French level is
152 much less than that of Spain, there seems to be no evidence of over-estimation of the transport
153 distance.

154

155 *4. The scientific methods and assumptions are generally both valid and clearly outlined? However,*
156 *when they filter the observational record, then they exclude stations with low amounts of pollen.*
157 *The threshold is 25 pollen day m⁻³. This is not appropriate. Stations with both high and low*
158 *numbers should be included in the evaluation of the model simulations.*

159 We respectfully disagree. As stated above, Hirst trap data are very uncertain for low pollen
160 concentrations. The uncertainty of daily (!) values is generally considered to be around 5-10 pollen
161 m⁻³. Therefore, our current filtering threshold is actually very soft.

162

163 *5. The results are not sufficient to support the interpretations and conclusions? This is partly*
164 *caused by the design of figures. As an example, Figure 3 shows simulated (maps) and observed*
165 *(dots) pollen index. The maps are good for a broad picture, but the accuracy at the sites cannot be*
166 *assessed with the maps. Ideally this should be combined with a table that demonstrate model results*
167 *vs observations. Figure 5 shows maps with observed start dates and the corresponding*
168 *calculations. The chosen color scale makes it almost impossible to see any variations. A difference*
169 *between 114 and 126 is from on type of green to another, but cover almost 14 days. This means that*
170 *differences and agreements between observations cannot be assessed to an accuracy of less than 14*
171 *days. A table would make this much more clear. Same arguments on accuracy assessments are*
172 *relevant for Figure 6. This would also have been better in a table. As the manuscript hardly uses*
173 *the spatial representation of the maps with the dots (Fig 3,5,6), then there is limited argument for*
174 *showing these comparisons on a map. Using tables instead of figures would therefore improve*
175 *transparency substantially.*

176 We have added supplementary table repeating the information provided by maps. Also, the color
177 legend was revised to improve the readability of the maps.

178

179 *The authors claim a strong forecasting skill in the summary. However Figure 7 clearly shows very*
180 *low correlations (from below 0.1 to less than 0.4) and the RMSE (also figure 7) ranges from about*
181 *80 grains/m³ to 120 grains/m³. As far as I know this level is the typical level for severe warnings of*

182 *tree pollen. If the typical error is of the same level as the warning level and the correlations*
183 *generally low, then I do not find sufficient support for the statement concerning a strong forecasting*
184 *skill.*

185 This is confusing: we do not claim strong forecasting skill in the summary. To the opposite, the
186 paper states “noticeable deviations from both observations and each other” in the abstract and
187 discusses the season shift in the summary. What concerns “decent level of reproduction of short-
188 term phenomena”, this is confirmed by the sensitivity runs: as soon as the season timing is crudely
189 corrected the correlation nearly doubles, thus suggesting that the short-term features of the time
190 series are fine. Therefore, we respectfully disagree with this criticism.

191

192 *6. The results cannot be reproduced by fellow scientists. The model simulations can be reproduced,*
193 *but the accuracy assessment cannot be done as there is no description of the observational record.*

194 Description of the observations is provided in the revised paper as a supplementary table

195

196 *7. The authors give credit to related work but it is my impression that they have not conducted a*
197 *sufficient literature review, in particular in relation to other modelling approaches that simulates*
198 *the start and the strength of the pollen season. This puts limitations to the scientific discussion of*
199 *the work and the assessment of the quality of the model simulations. A quick search on Google*
200 *identified studies by Orlandi et al (2006) and Rojo et al (2016). These studies in combination with*
201 *papers written by the co-authors of this manuscript (e.g. Galan et al, 2005) present methods that*
202 *seem to have similar or higher accuracy than this study with respect to start of the pollen season as*
203 *well as the spatial modelling of the season index. This indicates that a deeper literature review is*
204 *needed in order to position the findings in this manuscript against existing knowledge. The authors*
205 *claim a strong forecasting skill in the summary. However, all of the models (Figure 7), except*
206 *SILAM, seem to have a larger error with respect to predicting the start of the season than other*
207 *multi-site methods presented in scientific literature. It can therefore be questioned if there is a*
208 *strong forecasting skill of the models and the ensemble with respect to the start of the season.*

209 The topic of comparison of regional numerical transport models with local statistical models (even
210 if the latter ones are based on more than one station) is a large topic, which goes way beyond the
211 current exercise. We discussed it in several previous publications, in particular in recent Ritenberga
212 et al (2016), where showed that even for birch (the most-accurately modelled pollen type) the local
213 model outperforms SILAM. This is how it should be: European-scale models cannot be tuned to a

214 single place in principle, they would inevitably miss rest of Europe. In that sense, for instance,
215 better performance in Perugia of the model made in Perugia (Orlandi et al, 2006) is not surprising.
216 Corresponding discussion is added.

217 The Rojo et al (2016) paper does not concern the season forecasting, only static dependence of SPI
218 and source map. It is certainly an interesting work and we included it now but its findings are not
219 relevant for the time series analysis.

220 At the same time, in conclusions we highlight the large season shift as the matter of primary
221 importance, which calls for investigation and, possibly, reparameterization of the source term. And,
222 once again, conclusions did not contain the claim of strong forecasting skills of the ensemble.

223

224 *8. The title clearly reflects the contents of the paper*

225 *9. The abstract provides a concise summary of the study. However as described in the previous*
226 *sections, then there is not sufficient material in the manuscript to support the findings that are*
227 *presented in the abstract*

228 See responses to items 5, 6 and 7.

229

230 *10. The overall presentation is well structured and clear.*

231 *11. The language is fluent and precise*

232 *12. Equation 1 and 2 are defined. However the scaling factors and*

233 *are only partly described as their values could not be identified.*

234 The omissions are corrected. See response to the Referee 1

235

236 *13. The figures 3,5,6 are almost impossible to read causing that the findings presented in the*
237 *conclusion and abstract rely on unclear material*

238 The figure quality has been improved and the table material provided as a supplement.

239

240 *14. There is about 75 references. Most of these are peer reviewed literature. However a substantial*
241 *amount of the cited literature appear to be written (as lead or co-author) of the authors to this*
242 *manuscript. The comments under point number 7 and the large number of references indicates that*
243 *the authors of this manuscript had put too much weight on own publications and to little weight on*
244 *publications by other authors.*

245 The current work is a synthetic effort of the many groups playing key roles in the olive pollen
246 aerobiology. We did our best to provide adequate representation of other groups, further expanded
247 the literature review and discussion in the revised paper and included the extra references suggested
248 by the referee. However, one of the suggested papers was also co-authored by the authors of this
249 paper, and we have already quoted two works originated from the same group in the initial paper
250 version. Therefore, we reject the blame of the biased literature review.

251

252 *15. Supplementary material has not been included*

253

254

255

256

257

Formatted: Normal

258
259
260

261
262
263
264
265
266

267

268
269
270
271
272
273
274
275
276
277
278
279
280
281
282
283
284
285
286
287
288
289
290
291
292
293

294

Multi-model ensemble simulations of olive pollen
distribution in Europe in 2014: [current status and outlook](#).

Mikhail Sofiev¹, Olga Ritenberga², Roberto Albertini³, Joaquim Arteta⁴, Jordina Belmonte^{5,6}, [Carmi Geller Bernstein](#)⁷, Maira Bonini⁸, Sevcan Celenk⁹, Athanasios Damialis^{10,11}, John Douros¹², Hendrik Elbern¹³, Elmar Friese¹³, Carmen Galan¹⁴, Gilles Oliver¹⁵, Ivana Hrga¹⁶, Rostislav Kouznetsov¹, Kai Krajsek¹⁷, [Donat Magyar](#)¹⁸, Jonathan Parmentier⁴, Matthieu Plu⁴, Marje Prank¹, Lennart Robertson¹⁹, Birthe Marie Steensen²⁰, Michel Thibaudon¹⁵, Arjo Segers²¹, Barbara Stepanovich¹⁶, Alvaro M. Valdebenito²⁰, Julius Vira¹, Despoina Vokou¹¹

¹ Finnish Meteorological Institute, Erik Palmenin Aukio 1, Finland
² University of Latvia, Latvia
³ Department of [Medicine and Surgery](#), University of Parma, Italy
⁴ CNRM UMR 3589, Météo-France/CNRS, Toulouse, France
⁵ Institute of Environmental Sciences and Technology (ICTA), Universitat Autònoma de Barcelona, Spain
⁶ Depatment of Animal Biology, Plant Biology and Ecology, Universitat Autònoma de Barcelona, Spain
⁷ [Sheba Medical Center, Ramat Gan Zabludowicz Center for Autoimmune Diseases, Israel](#)
⁸ Agenzia Tutela della Salute della Città Metropolitana di Milano/ LHA ATS Città Metropolitana Milano, Italy
⁹ Biology department, Uludag University, Turkey
¹⁰ Chair and Institute of Environmental Medicine, UNIKA-T, Technical University of Munich and Helmholtz Zentrum München - German Research Center for Environmental Health, Augsburg, Germany
¹¹ Department of Ecology, School of Biology, Aristotle University of Thessaloniki, Greece
¹² Royal Netherlands Meteorological Institute, De Bilt, The Netherlands
¹³ Rhenish Institute for Environmental Research at the University of Cologne, Germany
¹⁴ University of Cordoba, Spain
¹⁵ RNSA, Brussieu, France
¹⁶ Andrija Stampar Teaching Institute of Public Health, Croatia
¹⁷ Institute of Energy and Climate Research (IEK-8), Forschungszentrum Jülich, Germany
¹⁸ [National Institute of Public Health, Hungary](#)
¹⁹ Swedish Meteorological and Hydrological Institute SMHI, Sweden
²⁰ MET Norway
²¹ TNO, Netherlands

Formatted: Normal

Deleted: 8

Deleted: 19

Deleted: 0

Deleted: 19

Deleted:

Deleted: Clinical and Experimental

Deleted: 8

Deleted: 19

Deleted: 0

304 1. Abstract

305 [The paper presents the first modelling experiment of the European-scale olive pollen dispersion,](#)
306 [analyses the quality of the predictions and outlines the research needs.](#) A 6-models strong ensemble
307 of Copernicus Atmospheric Monitoring Service (CAMS) was run through the season of 2014
308 computing the olive pollen distribution. The simulations have been compared with observations in 8
309 countries, members of the European Aeroallergen Network (EAN). Analysis was performed for
310 individual models, the ensemble mean and median, and for a dynamically optimized combination of
311 the ensemble members obtained via fusion of the model predictions with observations. The models,
312 generally reproducing the olive season of 2014, showed noticeable deviations from both
313 observations and each other. In particular, the season start was reported too early, by 8 days, but for
314 some models the error mounted to almost two weeks. For the season end, the disagreement between
315 the models and the observations varied from a nearly perfect match up to two weeks too late. A
316 series of sensitivity studies performed to understand the origin of the disagreements revealed crucial
317 role of ambient temperature [and consistency of its representation by the meteorological models and](#)
318 [by the heat-sum-based phenological model.](#) In particular, a simple correction to the heat sum
319 threshold eliminated the season-start shift but its validity in other years remains to be checked. The
320 short-term features of the concentration time series were reproduced better suggesting that the
321 precipitation events and cold/warm spells, as well as the large-scale transport were represented
322 rather well. Ensemble averaging led to more robust results. The best skill scores were obtained with
323 data fusion, which used the previous-days observations to identify the optimal weighting
324 coefficients of the individual model forecasts. Such combinations were tested for the forecasting
325 period up to 4 days and shown to remain nearly optimal throughout the whole period.

326

327 **Keywords:** olive pollen, airborne pollen modelling, pollen forecasting, multi-model ensemble, data
328 fusion, aerobiology

329

330 2. Introduction

331 Biogenic aerosols, such as pollen and spores, constitute a substantial fraction of particulate matter
332 mass in the air during the vegetation flowering season and can have strong health effects causing
333 allergenic rhinitis and asthma (G D'Amato et al., 2007). One of important allergenic trees is olive.

334 Olive is one of the most extensive crops and its oil is one of the major economic resources in
335 Southern Europe. The bulk of olive habitation (95% of the total area worldwide) is concentrated in
336 the Mediterranean basin (Barranco et al., 2008). Andalusia has by far the world's largest area given

Deleted: European

Deleted: persion in Europe

Deleted: 6

Deleted: , especially systematic biases in its representation by meteorological models

Deleted: A

Deleted: being

344 over to olive plantations, 62% of the total olive land of Spain and 15% of the world's plantations
345 (Gómez et al., 2014).

346 Olive pollen is also one of the most important causes of respiratory allergies in the Mediterranean
347 basin (G. D'Amato et al., 2007) and in Andalusia it is considered as the main cause of allergy. In
348 Cordoba City (S Spain), 71-73% of pollen-allergy sufferers are sensitive to olive pollen (Sánchez-
349 Mesa et al., 2005). (Cebrino et al., 2017). High rates of sensitization to olive pollen have been
350 documented in Mediterranean countries: 44% in Spain and 20% in Portugal (Pereira et al., 2006),
351 31.8% in Greece (Gioulekas et al., 2004), 27.5% in Portugal (Loureiro et al., 2005), 24% in Italy
352 (Negri et al., 1992), 21.6% in Turkey (Kalyoncu et al., 1995), and 15% in France (Spieksma,
353 1990). At the same time, relations between allergy and pollen concentrations is person- and case-
354 specific: allergen content of the pollen grains varies from year to year and day to day, as well as the
355 individual sensitivity of allergy sufferers (de Weger et al., 2013; Galan et al., 2013)

356 Olive is an entomophilous species that presents a secondary anemophily, favored by the agricultural
357 management during the last centuries. This tree is very well adapted to the Mediterranean climate
358 and tolerates the high summer and the low winter temperatures, as well as the summer drought,
359 characteristic for this climate.

360 Olive floral phenology is characterized by bud formation during summer, dormancy during autumn,
361 budburst in late winter, and flowering in late spring (Fernandez-Escobar et al., 1992; Galán et al.,
362 2005; García-mozo et al., 2006). Similar to some other trees, olive flowering intensity shows
363 alternated years with high and low or even no pollen production. The characteristic quasi-biannual
364 cycles are well visible in observations (Ben Dhiab et al., 2016; Garcia-Mozo et al., 2014). This
365 cycle, similar to other trees, e.g., birch, is not strict and is frequently interrupted showing several
366 years with similar flowering intensity (Garcia-Mozo et al., 2014). Such cyclic behavior is related to
367 the reproductive development, which is completed in two consecutive years. In the first year, the
368 bud vegetative or reproductive character is determined by the current harvest level, since this is the
369 main factor responsible for the inter-annual variation of flowering. In the second year, after the
370 winter rest, the potentially reproductive buds that have fulfilled their chilling requirements develop
371 into inflorescences (Barranco et al., 2008).

372 After the bud break, certain bio-thermic units are required for the development of the
373 inflorescences. Both the onset of the heat accumulation period and the temperature threshold for the
374 amount of positive heat units might vary according to the climate of a determined geographical
375 area. The threshold level was also reported to decrease towards the north (Aguilera et al., 2013).
376 Altitude is the topographical factor most influencing olive local phenology and the major weather

Field Code Changed

Deleted: many other

378 factors are temperature, rainfall, and solar radiation that control the plant evapotranspiration (Oteros
379 et al., 2013; Oteros et al., 2014).

380 Several studies used airborne pollen as a predictor variable for determining the potential sources of
381 olive pollen emission, e.g. Concentric Ring Method (J. Oteros et al., 2015; Rojo et al., 2016),
382 geostatistical techniques (Rojo and Pérez-Badia, 2015) and the spatio-temporal airborne pollen
383 maps (Aguilera et al., 2015).

384 There is a substantial variability of olive biological characteristics and its responses to
385 environmental stresses. In particular, the allergen content was shown to be strongly different in
386 pollen coming from different parts of the Iberian Peninsula (Galan et al., 2013).

387 Forecasting efforts of the olive pollen season were mainly concentrated on statistical models
388 predicting the season start and peak using various meteorological predictors. The bulk of studies is
389 based on information from one or a few stations within a limited region (e.g., Orlandi et al., (2006),
390 Moriondo et al., (2001), Alba and Diaz De La Guardia, (1998), Frenguelli et al., (1989), Galán et
391 al., (2005), Fornaciari et al., (1998), etc.). Several wider-area studies were also performed aiming at
392 more general statistical characteristics of the season, e.g. (Aguilera et al., 2014, 2013; Galan et al.,
393 2016).

394 Numerical modelling of olive pollen transport is very limited. In fact, the only regional-scale
395 computations regularly performed since 2008 were made by the SILAM model (<http://silam.fmi.fi>)
396 but the methodology was only scarcely outlined in (Galan et al., 2013).

397 Copernicus Atmospheric Monitoring Service CAMS (<http://atmosphere.copernicus.eu>) is one of the
398 services of the EU Copernicus program, addressing various global and regional aspects of
399 atmospheric state and composition. CAMS European air quality ensemble (Marécal et al., 2015)
400 provides high-resolution forecasts and reanalysis of the atmospheric composition over Europe.
401 Olive pollen is one of the components, which are being introduced in the CAMS European
402 ensemble in co-operation with European Aeroallergen Network EAN
403 (<https://www.polleninfo.org/country-choose.html>).

404 One of possible ways of improving the quality of model predictions without direct application of
405 data assimilation is to combine them with observations via ensemble-based data fusion methods
406 (Potemski and Galmarini, 2009). Their efficiency has been demonstrated for air quality problems
407 (Johansson et al., 2015 and references therein) and climatological models (Genikhovich et al., 2010)
408 but the technology has never been applied to pollen.

Deleted: (Oteros et al., 2015)

Field Code Changed

Deleted: (

Deleted: (

Deleted: (

Deleted: (

Field Code Changed

Field Code Changed

Deleted: (

Formatted: English (U.K.)

Deleted: izing the

Deleted: –

Field Code Changed

Deleted: (Aguilera et al., 2014)(Aguilera et al., 2013), (Galan et al., 2016)

419 The aim of the current publication is to present the first Europe-wide ensemble-based evaluation of
420 the olive pollen dispersion during the season of 2014. The study followed the approach of the multi-
421 model simulations for birch (Sofiev et al., 2015) with several amendments reflecting the peculiarity
422 of olive pollen distribution in Europe. We also made further steps towards fusion of model
423 predictions and observations and demonstrate its value in the forecasting regime.

424 The next section will present the participating models and setup of the simulations, the observation
425 data used for evaluation of the model predictions, approach for constructing an optimised multi-
426 model ensemble, and a list of sensitivity computations. The Results section will present the
427 outcome of the simulations and the quality scores of the individual models and the ensemble. The
428 Discussion section will be dedicated to analysis of the results, considerations of the efficiency of the
429 multi-model ensemble for olive pollen, and identification of the development needs.

430 3. Materials and methods

431 This section presents the regional models used in the study, outlines the olive pollen source term
432 implemented in all of them, and pollen observations used for evaluation of the model predictions.

433 3.1. Dispersion models

434 The dispersion models used in the study comprise the CAMS European ensemble, which is
435 described in details by Marécal et al., (2015) and (Sofiev et al., 2015). Below, only the model
436 features relevant for the olive pollen atmospheric transport calculations are described.

437 The ensemble consisted of six models.

438 **EMEP** model of EMEP/MSC-West (European Monitoring and Evaluation Programme /
439 Meteorological Synthesizing Centre - West) is a chemical transport model developed at the
440 Norwegian Meteorological Institute and described in Simpson et al., (2012). It is flexible with
441 respect to the choice of projection and grid resolution. Dry deposition is handled in the lowest
442 model layer. A resistance analogy formulation is used to describe dry deposition of gases, whereas
443 for aerosols the mass-conservative equation is adopted from Venkatram, (1978) with the dry
444 deposition velocities dependent on the land use type. Wet scavenging is dependent on precipitation
445 intensity and is treated differently within and below cloud. The below-cloud scavenging rates for
446 particles are based on Scott, (1979). The rates are size-dependent, growing for larger particles.

EURAD-IM (<http://www.eurad.uni-koeln.de>) is an Eulerian meso-scale chemistry transport model involving advection, diffusion, chemical transformation, wet and dry deposition and sedimentation of tropospheric trace gases and aerosols (Hass et al., 1995; Memmesheimer et al., 2004). It includes 3D-VAR and 4D-VAR chemical data assimilation (Elbern et al., 2007) and is able to run in nesting mode. The positive definite advection scheme of Bott (1989) is used to solve the advective transport and the aerosol sedimentation. An eddy diffusion approach is applied to parameterize the vertical sub-grid-scale turbulent transport (Holtslag and Nieuwstadt, 1986). Dry deposition of aerosol species is treated size-dependent using the resistance model of Petroff and Zhang (2010). Wet deposition of pollen is parameterized according to Baklanov and Sorensen (2001).

LOTOS-EUROS (<http://www.lotos-euros.nl/>) is an Eulerian chemical transport model (Schaap et al., 2008). The advection scheme follows Walcek and Aleksic (1998). The dry deposition scheme of Zhang et al. (2001) is used to describe the surface uptake of aerosols. Below-cloud scavenging is described using simple scavenging coefficients for particles (Simpson et al., 2003).

MATCH (<http://www.smhi.se/en/research/research-departments/air-quality/match-transport-and-chemistry-model-1.6831>) is an Eulerian multi-scale chemical transport model with mass-conservative transport and diffusion based on a Bott-type advection scheme (Langner et al., 1998; Robertson and Langner, 1999). For olive pollen, dry deposition is mainly treated by sedimentation and a simplified wet scavenging scheme is applied. The temperature sum, which drives pollen emission, is computed off-line starting from January onwards and is fed into the emission module.

MOCAGE (http://www.cnrm.meteo.fr/gmgec-old/site_engl/mocage/mocage_en.html) is a multi-scale dispersion model with grid-nesting capability (Josse et al., 2004; Martet et al., 2009). The semi-Lagrangian advection scheme of Williamson and Rasch (1989) is used for the grid-scale transport. The convective transport is based on the parameterization proposed by Bechtold et al. (2001) whereas the turbulent diffusion follows the parameterization of Louis (1979). Dry deposition including the sedimentation scheme follows Seinfeld and Pandis (1998). The wet deposition by the convective and stratiform precipitations is based on Giorgi and Chameides (1986).

SILAM (<http://silam.fmi.fi>) is a meso-to-global scale dispersion model (Sofiev et al., 2015), also described in the review of Kukkonen et al. (2012). Its dry deposition scheme (Kouznetsov and Sofiev, 2012) is applicable for a wide range of particle sizes including coarse aerosols, which are primarily removed by sedimentation. The wet deposition parameterization distinguishes between sub- and in-cloud scavenging by both rain and snow (Sofiev et al., 2006). For coarse particles, impaction scavenging parameterised following (Kouznetsov and Sofiev, 2012) is dominant below the cloud. The model includes emission modules for six pollen types: birch, olive, grass, ragweed,

480 mugwort, and alder, albeit only birch, ragweed, and grass sources are so-far described in the
481 literature (Prank et al., 2013; Sofiev, 2016; Sofiev et al., 2012).

482 Three **ENSEMBLE** models were generated by (i) arithmetic average, (ii) median and (iii) optimal
483 combination of the 6 model fields. Averaging and median were taken on hourly basis, whereas
484 optimization was applied at daily level following the temporal resolution of the observational data.
485 For the current work, we used simple linear combination c_{opt} of the models c_m , $m=1..M$ minimising
486 the regularised RMSE J of the optimal field:

$$487 \quad (1) \quad c_{opt}(i, j, k, t, \tau, A) = a_0(\tau) + \sum_{m=1}^M a_m(\tau) c_m(i, j, k, t), \quad A = [a_1..a_M], \quad a_m \geq 0 \quad \forall m$$

$$488 \quad (2) \quad J(t, \tau) = \sqrt{\frac{1}{O} \sum_{o=1}^O \left(c_{opt}(i_o, j_o, k_o, t, \tau, A) - c_o(t) \right)^2} +$$

$$\alpha \sum_{m=1}^M \left(a_m(\tau) - \frac{1}{M} \right)^2 + \beta \sum_{m=1}^M \left(a_m(\tau-1) - a_m(\tau) \right)^2, \quad \tau = \{d_{-k}, d_0\}$$

489 Here, i, j, k, t are indices along the x, y, z, and time axes, M is the number of models in the ensemble, O
490 is the number of observation stations, $\tau = \{d_{-k}:d_0\}$ is the time period of $k+1$ days covered by the
491 analysis window, starting from d_{-k} until d_0 , $\tau-1$ is the previous-day analysis period $\tau-1 = \{d_{-k-1}:d_{-1}\}$,
492 c_m is concentration of pollen predicted by the model m , [c_o is observed pollen concentration](#), a_m is
493 time-dependent weight coefficient of the model m in the ensemble, [a₀ is time-dependent bias](#)
494 [correction](#). In the Eq. (2), the first term represents the RMSE of the assimilated period τ , the second
495 term limits the departure of the coefficients from the homogeneous weight distribution, the third
496 one limits the speed of evolution of the a_m coefficients in time. The scaling values α and β decide
497 on the strength of regularization imposed by these two terms.

498 The ensemble was constructed mimicking the forecasting mode. Firstly, the analysis is made using
499 data from the analysis period τ . The obtained weighting coefficients a_i are used over several days
500 forwards from day d_0 : from d_1 until d_{nf} , which constitute the forecasting steps. The performance of
501 the ensemble is evaluated for each length of the forecast, from 1 to n_f days.

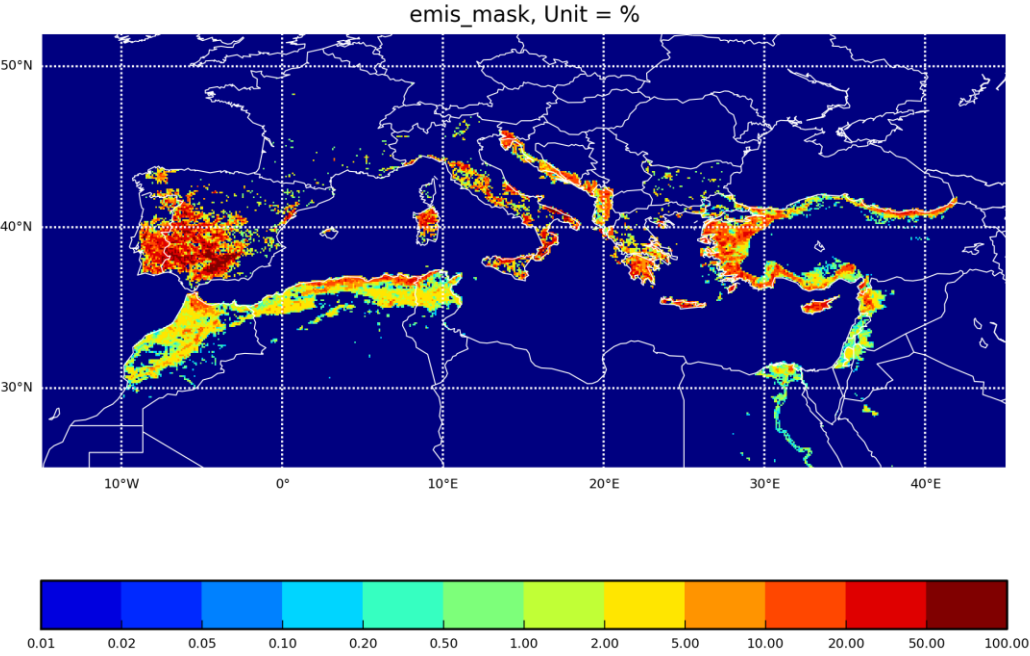
502 3.2. Olive pollen source term

503 All models of this study are equipped with the same olive pollen source term, which has not been
504 described in the scientific literature yet. However, it follows the same concept as the birch source
505 (Sofiev et al., 2012) that was used for the birch ensemble simulations (Sofiev et al., 2015). The

506 formulations and input data are open at <http://silam.fmi.fi/MACC>. The main input dataset is the
507 annual olive pollen production map based on ECOCLIMAP dataset (Champeaux et al., 2005;
508 Masson et al., 2003), Figure 1.

509 ECOCLIMAP incorporates the CORINE land-cover data for most of western-European countries
510 with explicit olive-plantations land-use type (CEC, 1993). For Africa and countries missing from
511 CORINE, the empty areas were filled manually assuming that 10% of all tree-like land-use types
512 are olives. This way, Tunisian, Egyptian, and Algerian olive plantations were recovered and
513 included in the inventory. In some areas, such as France (Figure 1), the olive habitat looks
514 unrealistically low, probably because the large olive plantations are rare but the trees are planted in
515 private gardens, city park areas, streets, etc. Since these distributed sources are not reflected in the
516 existing land-use inventories, they are not included in the current pollen production map.

517

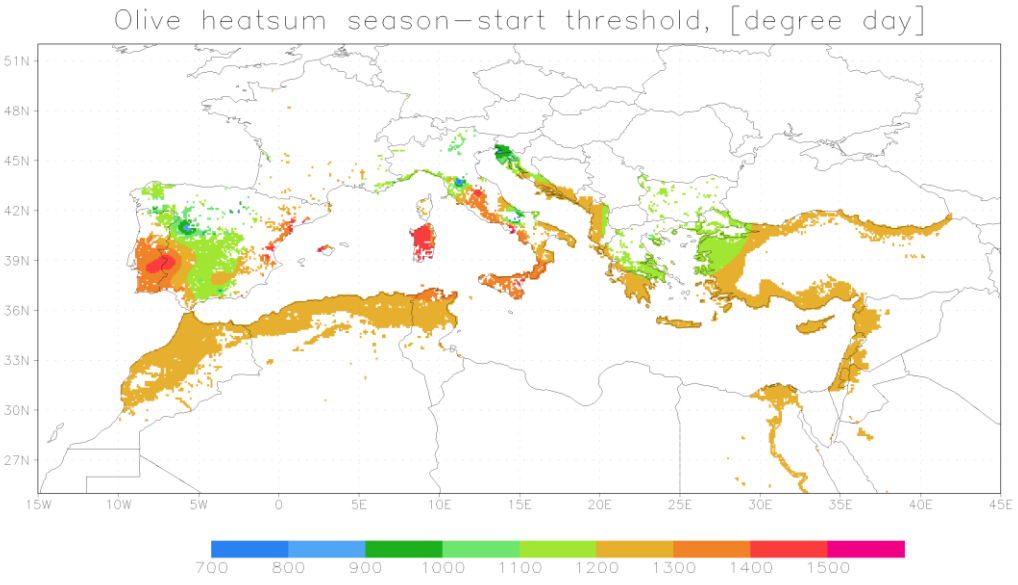


519 **Figure 1.** Olive pollen habitat map, percentage of the area occupied by the trees, [%]. Productivity of an area with
520 100% olive coverage is assumed to be 10^{10} pollen grain m^{-2} season $^{-1}$.

521

522 Similar to birch, the flowering description follows the concept of Thermal Time phenological
523 models and, in particular, the double-threshold air temperature sum approach of Linkosalo et al.

524 (2010) modified by Sofiev et al. (2012). Within that approach, the heat accumulation starts on a
525 prescribed day in spring (1 January in the current setup – after Spano et al. (1999), Moriondo et al.
526 (2001), Orlandi et al. (2005a, 2005b) and continues throughout spring. The cut-off daily
527 temperature below which no summation occurs is 0°C, as compares to 3.5°C for birch, was
528 obtained from the multi-annual fitting of the season start. Flowering starts when the accumulated
529 heat reaches the starting threshold (Figure 2) and continues until the heat reaches the ending
530 threshold (in the current setup, equal to the start-season threshold + 275 degree day). The rate of
531 heat accumulation is the main controlling parameter for pollen emission: the model assumes direct
532 proportionality between the flowering stage and fraction of the heat sum accumulated to-date.



533 GrADS: COLA/IGES 2016-12-13-10:57

534 **Figure 2.** Heat sum threshold for the start of the season. Unit = [degree day]

535

536 Similar to birch parameterization of Sofiev et al. (2012), the model distinguishes between the pollen
537 maturation, which is solely controlled by the heat accumulation described above, and pollen release,
538 which depends on other parameters. Higher relative humidity (RH) and rain reduce the release,
539 completely stopping it for $RH > 80\%$ and/or $rain > 0.1 \text{ mm hr}^{-1}$. Strong wind promotes it by up to
540 50%. Atmospheric turbulence is taken into account via the turbulent velocity scale and thus
541 becomes important only in cases close to free convection. In stable or neutral stratification and calm

542 conditions the release is suppressed by 50%. The interplay between the pollen maturation and
543 release is controlled by an intermediate ready-pollen buffer, which is filled-in by the maturation and
544 emptied by the release flows.

545 Local-scale variability of flowering requires probabilistic description of its propagation (Siljamo et
546 al., 2008). In the simplest form, the probability of an individual tree entering the flowering stage can
547 be considered via the uncertainty of the temperature sum threshold determining the start of
548 flowering for the grid cell – 10% in the current simulations. The end of the season is described via
549 the open-pocket principle: the flowering continues until the initially available amount of pollen is
550 completely released. The uncertainty of this number is taken to be 10% as well.

551

552 3.3.Pollen observations

553 The observations for the model evaluation in 2014 have been provided by the following 6 national
554 networks, members of the European Aeroallergen Network (EAN): Croatia, Greece, France,
555 Hungary, Israel, Italy, Spain, and Turkey. The data were screened for completeness and existence of
556 non-negligible olive season: (i) time series should have at least 30 valid observations, (ii) at least 10
557 daily values during the season should exceed 3 pollen m⁻³, and (iii) the seasonal pollen index (SPI,
558 an integral of the concentrations over the whole season) should be at least 25 pollen day m⁻³. After
559 this screening, information of 62 sites was used in the intercomparison. Data from Hungary referred
560 to 2016 and required dedicated computations for evaluating the long-range transport events.

Deleted: 0

561 Pollen monitoring was performed with Burkard 7-day and Lanzoni 2000 pollen traps based on the
562 Hirst design (Hirst, 1952). The pollen grains were collected at an airflow rate of 10 l min⁻¹. The
563 observations covered the period from March until September, with some variations between the
564 countries. Daily pollen concentrations were used. Following the EAS-EAN requirements (Galán et
565 al., 2014; Jäger et al., 1995), most samplers were located at heights of between 10m and 30m on the
566 roofs of suitable buildings. The places were frequently downtown of the cities, i.e. largely represent
567 the urban-background conditions (not always though). With regard to microscopic analysis, the
568 EAS-EAN requirement is to count at least 10% of the sample using horizontal or vertical strips
569 (Galán et al., 2014). The actual procedures vary between the countries but generally comply. The
570 counting in 2014 was mainly performed along four horizontal traverses as suggested by Mandrioli
571 et al., (1998). In all cases, the data were expressed as mean daily concentrations (pollen m⁻³).

Deleted: s

3.4. Setup of the simulations

Simulations followed the standards of CAMS European ensemble (Marécal et al., 2015). The domain spanned from 25°W to 45°E and from 30°N to 70°N. Each of the 6 models was run with its own horizontal and vertical resolutions, which varied from 0.1° to 0.25° of the horizontal grid cell size, and had from 3 up to 52 vertical layers within the troposphere (Table 1). This range of resolutions is not designed to reproduce local aspects of pollen distribution, instead covering the whole continent and describing the large-scale transport. The 10km grid cells reach the sub-city scale but still insufficient to resolve the valleys and individual mountain ridges. The limited number of vertical dispersion layers used by some models is a compromise allowing for high horizontal resolution. Thick layers are not a major limitation as long as the full vertical resolution of the input meteorological data is used for evaluation of dispersion parameters (Sofiev, 2002).

The simulations were made retrospectively for the season of 2014 starting from 1 January (the beginning of the heat sum accumulation) until 30 June when the pollen season was over. All models produced hourly output maps with concentrations at 8 vertical levels (near surface, 50, 250, 500, 1000, 2000, 3000 and 5000 metres above the surface), as well as dry and wet deposition maps.

All models considered pollen as an inert water-insoluble particle 28 µm in diameter and with a density of 800 kg m⁻³.

Deleted: events

Deleted: ¶

Formatted: Space Before: 0 pt, Line spacing: single

Table 1. Setup of the simulations for the participating models

Model	Horizontal dispersion grid	Dispersion vertical	Meteo input	Meteo grid	Meteo vertical
EMEP	0.25° × 0.125°	20 levels up to 100 hPa	ECMWF IFS 00 operational forecast, internal preprocessor	0.25° × 0.125°	IFS lvs 39 – 91 up to 100 hPa
EURAD-IM	15 km, Lambert conformal proj.	23 layers up to 100 hPa	WRF based on ECMWF IFS	Same as CTM	Same as CTM
LOTOS-EUROS	0.25° × 0.125°	3 dyn. lys up to 3.5km, sfc 25m	ECMWF IFS 00 operational forecast, internal preprocessor	0.5° × 0.25°	IFS lvs 69-91 up to 3.5km
MATCH	0.2° × 0.2°	52 layers up to 7 km	ECMWF IFS 00 from MARS, internal preprocessor	0.2° × 0.2°	IFS vertical: 91 lvs
MOCAGE	0.2° × 0.2°	47 layers up to 5hPa (7 in ABL)	ECMWF IFS 00 operational forecast, internal preprocessor	0.125° × 0.125°	IFS vertical 91 lvs
SILAM	0.1° × 0.1°	9 layers up to 7.5 km	ECMWF IFS 00 operational forecast, internal preprocessor	0.125° × 0.125°	IFS lvs 62-137 up to ~110hPa

597 4. Results for the pollen season of 2014

598 4.1. Observed peculiarities of the season

599 At French Mediterranean stations (Aix-en-Provence, Avignon, Montpellier, Nice, Nîmes and
600 Toulon), the mean value of ~~the~~ Seasonal Pollen Index (SPI) ~~in 2014~~ was quite similar to that of
601 2012 but lower than in 2013 (~~see~~ (de Weger et al., 2013) ~~for the SPI relevance to allergy~~).

Deleted: 2014

Deleted: for olive tree

602 The start of the pollen season was earlier than in the previous five years. The duration of the season
603 has been the longest one on Aix-en-Provence, Nice and Nîmes since 2010. On Ajaccio (Corsica)
604 station, the SPI was higher in 2014 than at other stations, similar to the situation in 2012.

605 In Andalusia, 2014 was the second warmest year during the last decades but more humid than usual,
606 5% above the typical relative humidity level (<https://www.ncdc.noaa.gov/sotc/global/201413>).
607 However, after an intense olive flowering in 2013, in 2014 the flowering intensity was lower and
608 similar to 2012, in agreement with the bi-annual alterations of the season severity.

609 In Northern Italy, the 2014 olive pollen season was less intense than the average of the previous ten
610 years (2004-2013). Instead, in Southern Italy, the 2014 season was more intense in the first part and
611 less intense in the second part (after the beginning of June) than during previous seasons. No
612 differences were noted ~~with~~ respect ~~to~~ the start and the end of the season in both cases.

613 In Thessaloniki, Greece, in 2014, the pollen season started in the same time as during the last
614 decades (first half of April), but ended about 1.5 month later (last half of October). The pollen
615 season peak has been steadily in May. The SPI was considerably higher in 2014 (418 pollen day m⁻³
616 ³), compared against the previous two years (approximately 300 pollen day m⁻³). The overall shape
617 of the pollen season in 2014 resembled the ones during the last decade, however, with a multi-
618 modal and less peaky pattern.

619

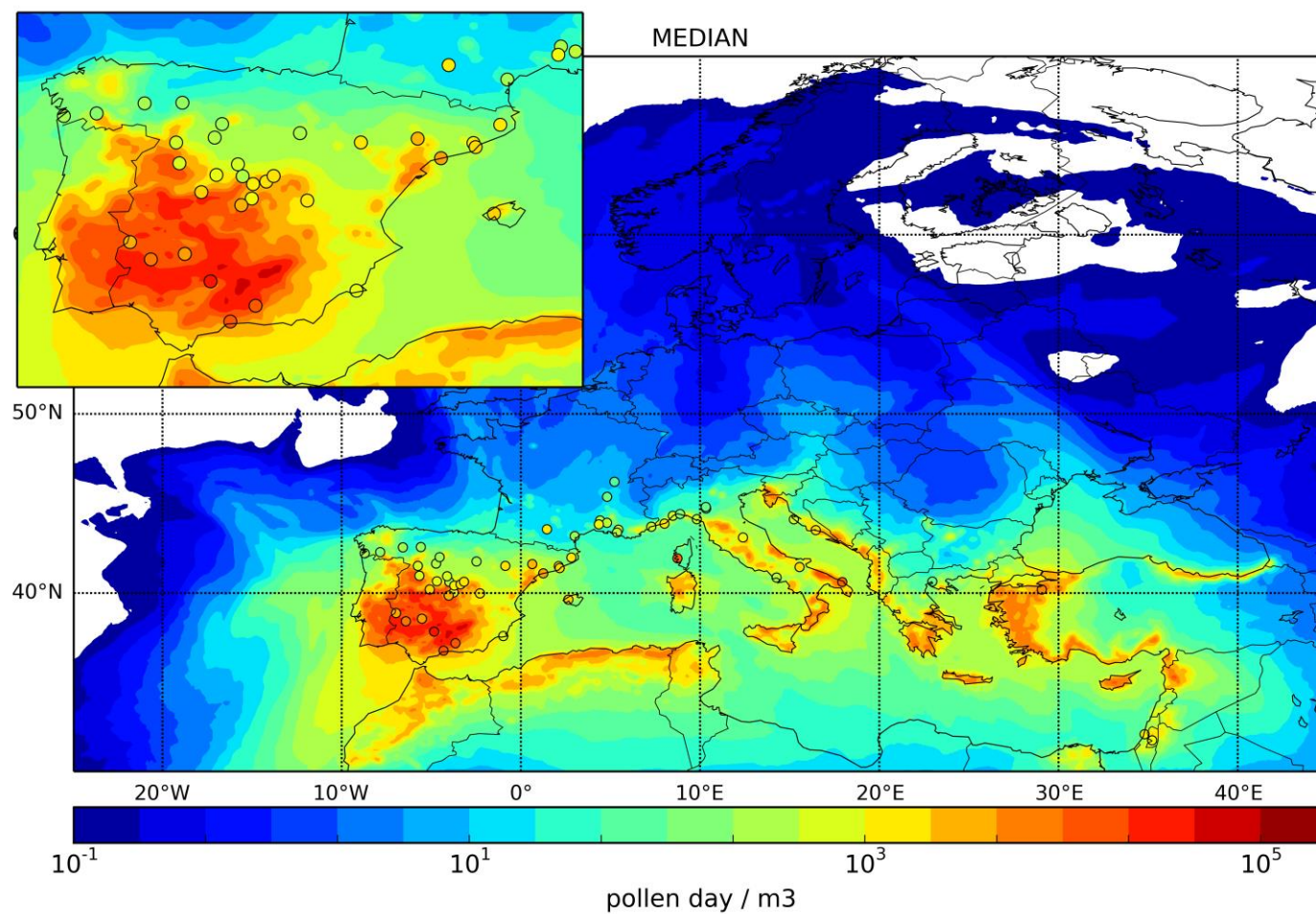


Figure 3. Observed (dots) and MEDIAN-model predicted (shades) Seasonal Pollen Index (SPI, sum of daily concentrations), 2014, [pollen day m⁻³].

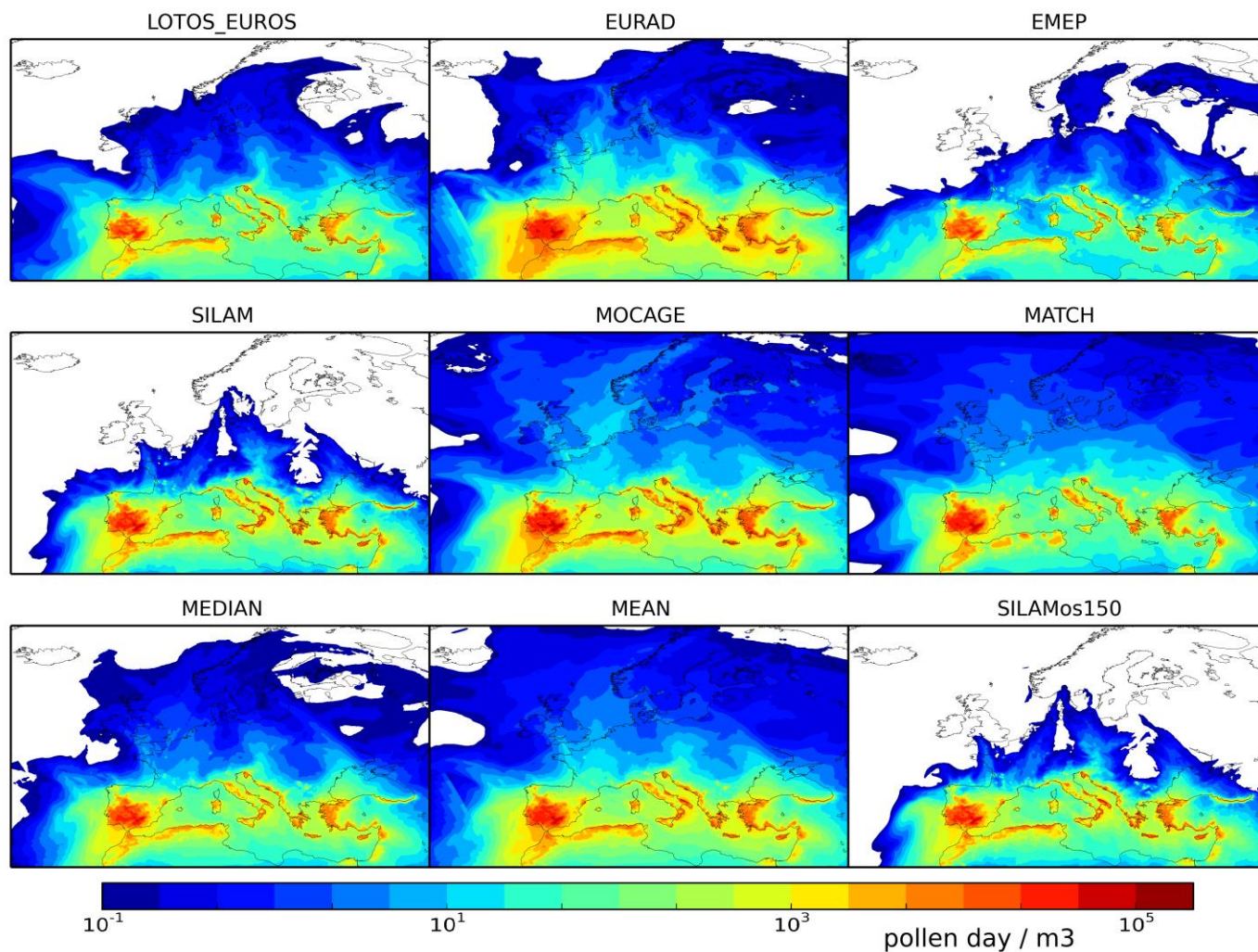


Figure 4. Modelled Seasonal Pollen Index (SPI) by the individual ensemble members and mean models, 2014, [pollen day m^{-3}].

Deleted: Observed (dots) and m

Deleted: o

Deleted: (shades)

Deleted: , sum of daily concentrations)

4.2. Model results

The total seasonal olive pollen load (Figure 3, Figure 4) expectedly correlates with the map of olive plantations (Figure 1), which is also confirmed by the observations (Figure 3). The highest load is predicted over Spain and Portugal, whereas the level in the Eastern Mediterranean is not so high reflecting smaller size of the areas covered by the olive trees and limited long-range transport over Mediterranean. The model predictions differ up to a factor of a few times (Figure 4), reflecting the diversity of modelling approaches, especially the deposition and vertical diffusion parameterizations (see Table 1 and section 3.1).

Since the olive plantations are located within a comparatively narrow climatic range, flowering propagates through the whole region within a few weeks starting from the coastal bands and progressing inland (not shown).

Deleted: Figure 4

Deleted: Figure 4

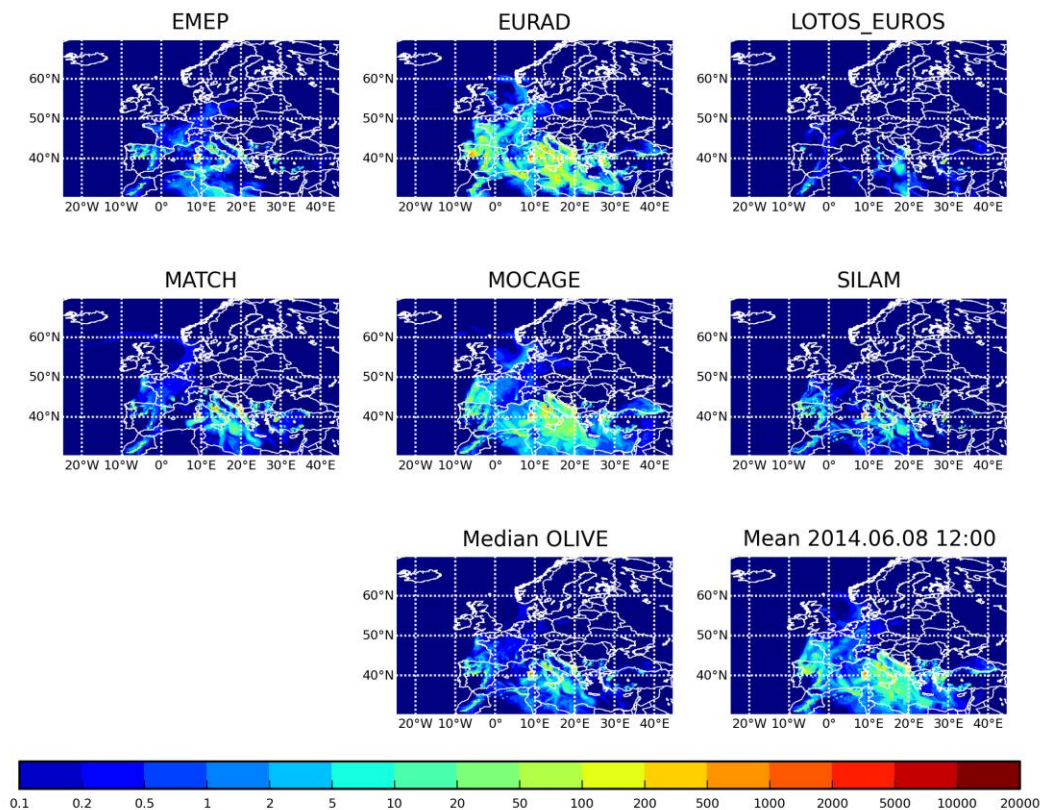


Figure 5. Example of hourly olive pollen concentrations, 12 UTC 08.06.2014, [pollen m^{-3}].

647

648 Hot weather during the flowering season leads to strong vertical mixing and deep atmospheric
649 boundary layer (ABL), which in turn promotes the pollen dispersion. As seen from Figure 5, the
650 pollen plumes can reach out over the whole Mediterranean and episodically affect Central Europe.
651 Both Figure 4 and Figure 5 illustrate the differences between the models, e.g. substantially higher
652 concentrations reported by EURAD-IM and MOCAGE as compared to other models. What regard
653 to pollen transport, the shortest transport with the fastest deposition is manifested by LOTOS-
654 EUROS (also, showed the lowest concentrations), while the longest one is suggested by MOCAGE.

655 The most-important general parameters describing the season timing are its start and end (Figure 6).
656 Following Andersen (1991), these dates are computed as dates when 5% and 95% of the SPI are
657 reached.

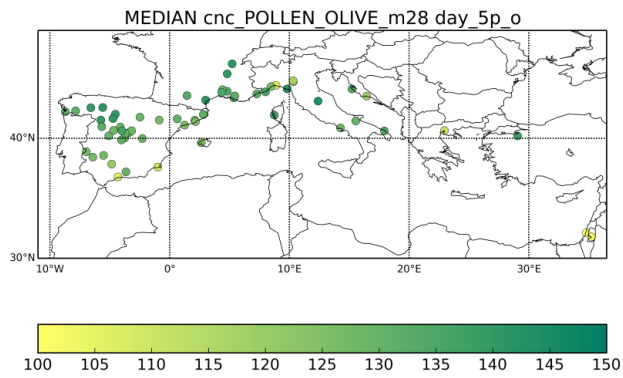
658 Computations of the model-measurement comparison statistics faces the problem of non-
659 stationarity and non-normal distribution of the daily pollen concentrations (Ritenberga et al., 2016).
660 For such processes, usual non-parametric statistics have to be taken with high care since their basic
661 assumptions are violated. Nevertheless, they can be formally calculated for both individual models
662 and the ensemble (Figure 7, Figure 8). The main characteristic of the ensemble, the discrete rank
663 histogram and the distribution of the modelled values for the below-detection-limit observations
664 (Figure 9) show that the spread of the obtained ensemble is somewhat too narrow in comparison
665 with the dynamic range of the observations. The same limitation was noticed for the birch
666 ensemble.

667 The patterns in Figure 6 and Figure 7 reveal a systematic early bias of the predicted season start and
668 end, which is well seen from normalised cumulative concentration time series (Figure 10). This bias
669 is nearly identical for all models, except for EURAD-IM, which also shows higher correlation
670 coefficient than other models. The reasons for the problem and for the diversity of the model
671 response are discussed in the next section.

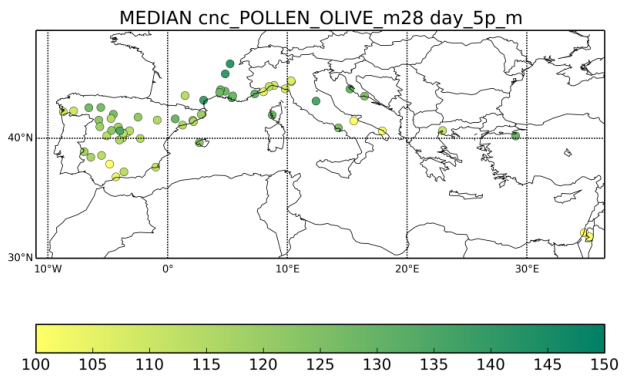
Field Code Changed

Deleted: Olga

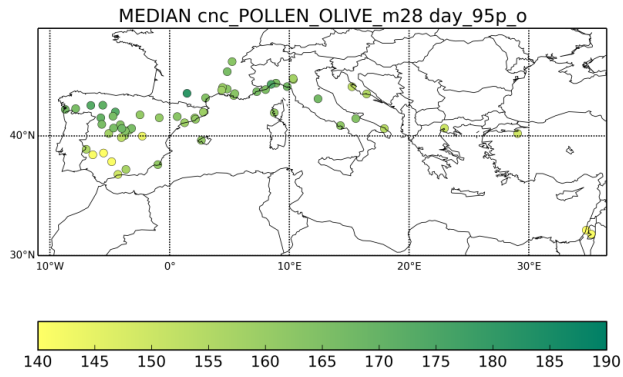
673



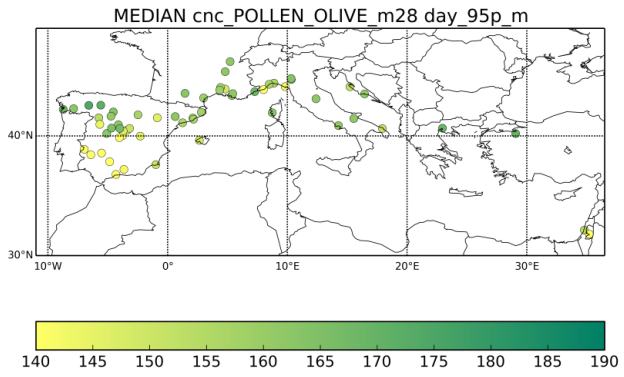
Season start day, 5%, observed



Season start day, 5%, ensemble median



Season end day, 95%, observed



Season end day, 95%, ensemble median

674

675

676

677

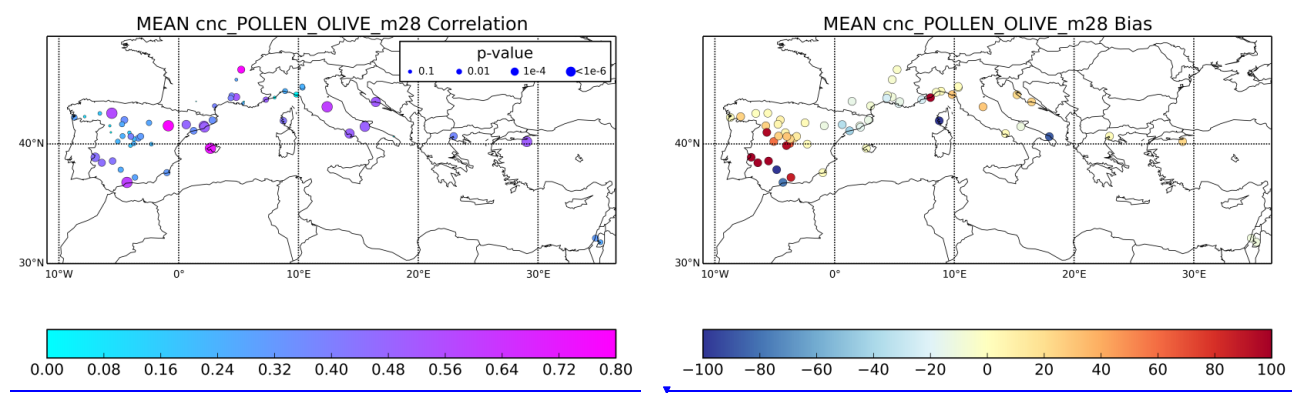
Figure 6. The start (date of 5% of the cumulative seasonal concentrations) and the end (95% of the cumulative seasonal concentrations) of the olive season in 2014 as day of the year, predicted by the median of the ensemble and observed by the stations with sufficient amount of observations.

Deleted: ¶

Formatted: Space Before: 0 pt, Line spacing: single

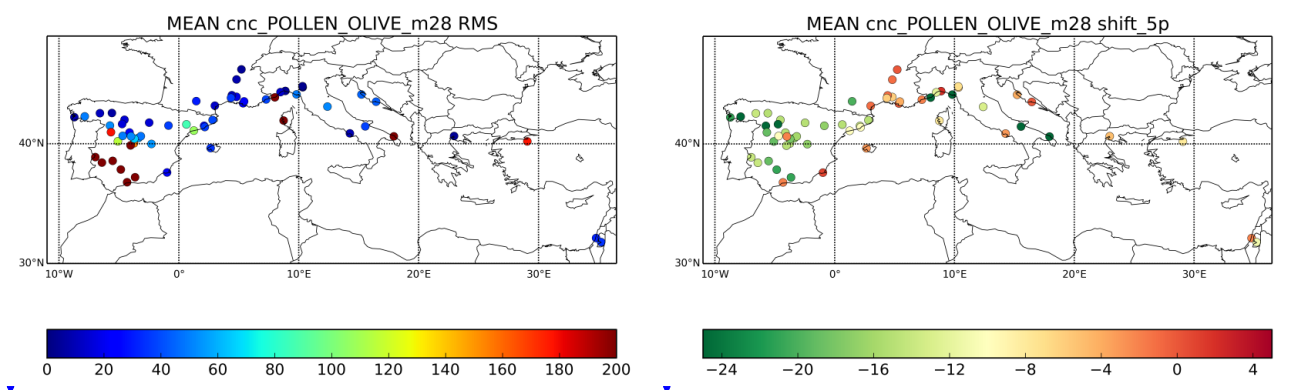
Formatted: Font: 4 pt

Formatted: Space Before: 0 pt, Line spacing: single



Correlation coefficient, dot size refers to p-value

Absolute bias, mean April-June, [pollen m⁻³]



RMSE, [pollen m⁻³]

Error in the season start, days

Figure 7. Results of model-measurement comparison for the ensemble mean: correlation coefficient for daily time series, mean bias April-June (pollen m⁻³), RMSE (pollen m⁻³), error in the season start (days).

Deleted: 1

MEAN cnc_POLLEN

Deleted:

MEAN cnc_POLLEN

Deleted:

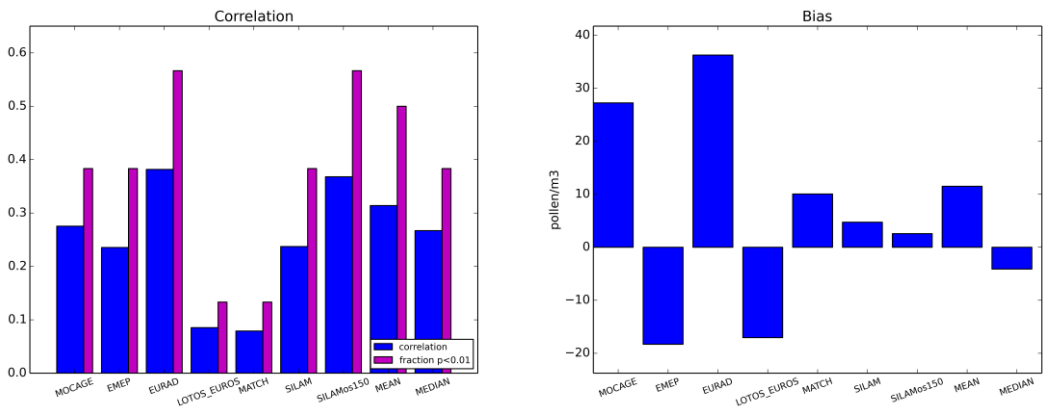
MEAN cnc_POLLEN

Deleted:

Formatted: Space Before: 0 pt, Line spacing: single

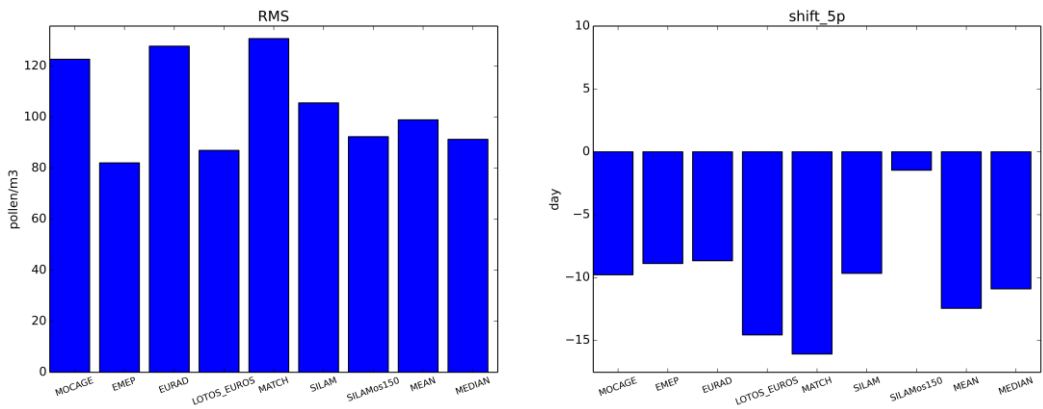
Formatted: Space Before: 0 pt, Line

695



Correlation coefficient and fraction of $p < 0.01$

Absolute bias, mean April-June [pollen m⁻³]



RMSE, [pollen m⁻³]

Error in the season start, days

696

697 **Figure 8.** Scores of the individual models, mean over all stations. The same parameters as in **Figure 7**. The sensitivity
698 run SILAMos150 is explained in the discussion section

699

700

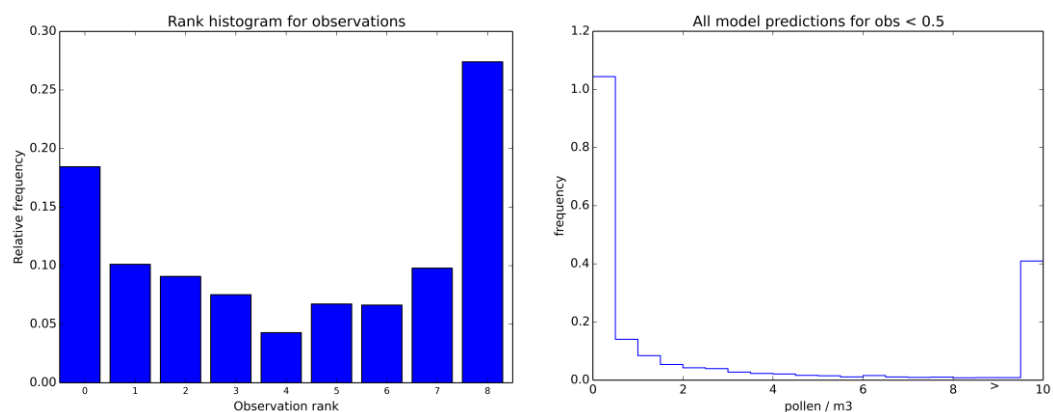


Figure 9. Ensemble characteristics. Left: discrete rank histogram for the constructed ensemble (daily concentration statistics); right: histogram of model predictions when observations were below the detection limit 0.5 pollen m⁻³,

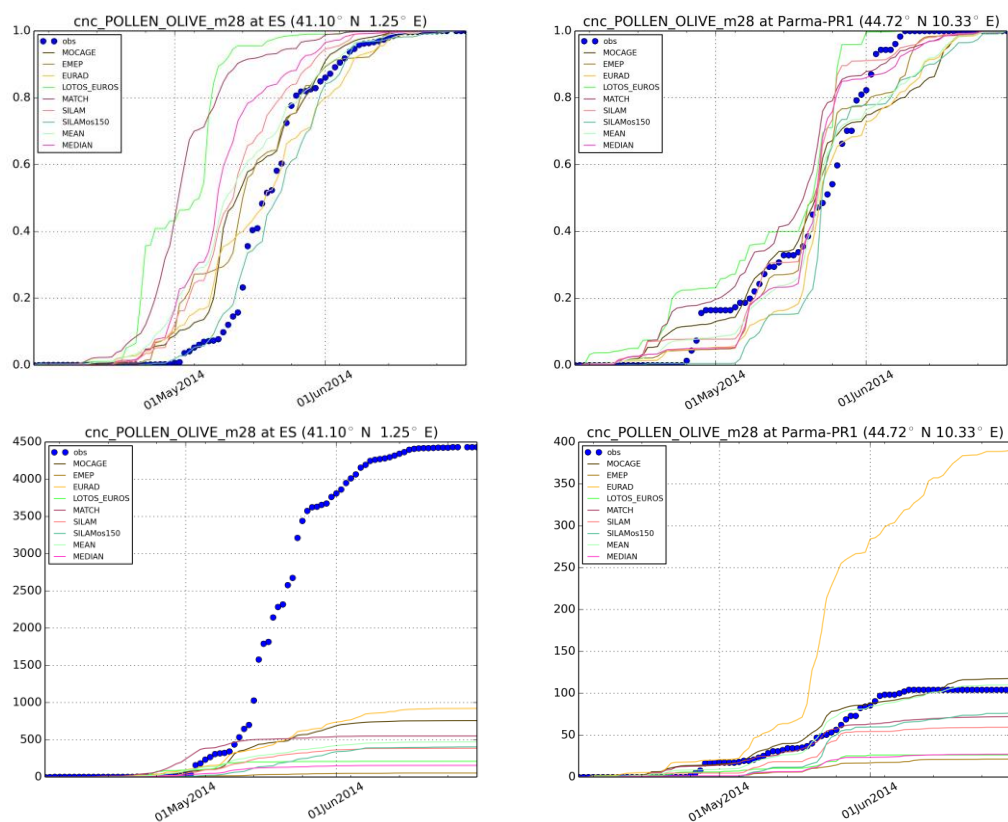


Figure 10. Cumulative time series of olive concentrations at Tarragona (Spain) and Parma (Italy). Upper row: normalized to the seasonal SPI [relative unit], lower: absolute cumulative concentrations [pollen day m⁻³].

708 5. Discussion

709 In this section, we consider the key season parameters and the ability of the presented ensemble to
710 reproduce those (section 5.1), the added value of the multi-model ensembles, including the
711 optimized ensemble (section 5.2), the main uncertainties that limit the model scores (section 5.3),
712 and the key challenges for future studies (section Error! Reference source not found.).

Deleted: the added value of the multi-model ensembles, including the optimized ensemble (section 5.2)

713 5.1. Forecast quality: model predictions for the key season parameters

714 The key date of the pollen season is its start: this very date refers to adaptation measures that need
715 to be taken by allergy sufferers. Predicting this date for olives is a significantly higher challenge
716 than, e.g., for birches: the heat sum has to be accumulated starting from 1 January with the season
717 onset being in mid-April, whereas for birches it is 1 March and mid-March, respectively. As a
718 result, prediction of the olive season start strongly depends on the temperature predictions by the
719 weather prediction model and the way this temperature is integrated into the heat sum.
720 Inconsistency between these, even if small, over the period of almost 4 months can easily lead to a
721 week of an error. As one can see from Figure 8 and Figure 7, there is a systematic, albeit spatially
722 inhomogeneous bias of all models by up to 10 days (too early season). Exception is the
723 SILAMos150 sensitivity run, which used the higher heat sum threshold, by 150 degree-days
724 (~10%), than the standard level (Figure 2). No other sensitivity runs, including the simulations
725 driven by ERA-Interim fields, showed any significant improvement of this parameter. Importantly,
726 EURAD-IM, which is driven by WRF meteo fields, also showed a similar bias. Finally, the shift
727 varies among the stations: from near-zero (France, some sites in Italy, Croatia, Greece, and Israel)
728 up to almost three weeks in North-Western Spain. It means that no “easy” solution exists and calls
729 for an analysis of long-term time series, aiming at refinement of the heat sum formulations and
730 threshold values.

Deleted: Bias

Deleted: the winter and spring

Deleted: bias of all models by about 8

Deleted: higher

Deleted: This

731 The end of the season showed an intriguing picture: EURAD-IM, despite starting the season as
732 early as all other models, ends it 2 days too late instead of 5 days too early as all other models (see
733 examples for two stations in Figure 10). This indicates that WRF, in late spring, predicts lower
734 temperature than IFS, which leads to longer-than-observed season in the EURAD-IM predictions.
735 Other models showed correct season length and, due to initial early bias, end it a few days too early.
736 The de-biased run SILAMos150 run shows almost perfect shape and hits both start and end with 1
737 day accuracy, which supports 250 degree day as a season length parameter.

Deleted: A certain daytime cold bias of WRF in late spring and summer has already been noticed at German measurement sites, which corroborates well with this finding.

750 The most-diverged model predictions are shown for the absolute concentrations (Figure 8). With the
751 mean observed April-June concentration of 35 pollen m⁻³ the range of predictions spans over a
752 factor of four: EURAD-IM and MOCAGE being twice higher and EMEP and LOTOS-EUROS
753 twice lower. Shifting the season by 5 days in the SILAMos150 run also changes the model bias,
754 reflecting differences in the transport patterns and the impact of stronger vertical mixing in later
755 spring. Spatially, the bias is quite homogeneous, except for southern Spain, where heterogeneous
756 pattern is controlled by local conditions at each specific site (Figure 7).

757 Temporal correlation is generally high in coastal areas (Figure 7) but at or below 0.5 in terrestrial
758 stations of Iberian Peninsula (the main olive plantations). This is primarily caused by the shifted
759 season: the simulations with more accurate season showed the highest correlation among all models
760 with ~60% of sites with significant correlation (p<0.01, Figure 8).

761 Comparison with local statistical models made for single or a few closely-located stations
762 expectedly shows that local models are usually comparable but somewhat more accurate (at their
763 locations) than the European-scale dispersion models (see also discussion in (Ritenberga et al.,
764 2016)). Thus, (Gala et al., 2001), analyzed performance of three popular local models for Cordoba,
765 with the best one showing the mean error of the start of the season of 4.7 days but reaching up to 14
766 days in some years. Similar error was found for Andalusia (Galán et al., 2005) and two sites
767 (Perugia and Ascoli Piceno) in Italy (Frenguelli et al., 1979) – 4.8 and 4.33 days of the standard
768 error, respectively. A recent study (Aguilera et al., 2014) constructed three independent statistical
769 models for Spain, Italy and Tunisia and ended up with over 5 days of a standard error for the
770 Mediterranean. In another study, the authors admitted the scale of the challenges: “The specific
771 moment for the onset of the olive heat accumulation period is difficult to determine and has
772 essentially remained unknown” (Aguilera et al., 2013).

773 One of the strengths of continental-scale dispersion models is their ability to predict long-range
774 transport events. However, direct evaluation of this feature for olive pollen is difficult since
775 countries without olive plantations usually do not count its pollen. One can however refer to Figure
776 3, (zoomed map of Spain), which shows that the ensemble successfully reproduces the drastic
777 change of the SPI from nearly 10⁵ pollen day m⁻³ in the south of Spain down to less than 100 pollen
778 day m⁻³ in the north. Episode-wise, an example of a well-articulated case of olive pollen transport
779 from Italy to Hungary in 2016 was brought up by Udvardy et al., (2017), who analyzed it with
780 adjoint SILAM simulations. The episode was also well-predicted by the forward computations.

Field Code Changed

Deleted: O.

Formatted: English (U.K.)

Field Code Changed

Formatted: English (U.K.)

Formatted: English (U.K.)

Deleted: Figure 3

Deleted: (

5.2. Ensemble added value

Arguably the main uncertainty of the model predictions was caused by the shift of the season start and end – the parameters heavily controlled by temperature, i.e. least affected by transport features of the models. As a result, application of the “simple” ensemble technologies does not lead to a strong improvement. Some effect was still noticed but less significant than in case of birch or traditional AQ forecasting. Therefore, in this section we also consider a possibility of ensemble-based fusion of the observational data with the model predictions. All ensembles were based on operational models, i.e. the SILAMos150 run was not included in either of them.

5.2.1. Mean ensembles: arithmetic average and median

Considering the mean-ensemble statistics, one should keep in mind that both the meteorological driver and the source term parameterization were the same for all models (except for EURAD driven by WRF). This resulted in the under-representative ensemble (Figure 9), where several good and bad features visible in all models propagate to the mean ensembles.

Among the simple means, arithmetic average performed better than the median, largely owing to strong EURAD-IM impact. That model over-estimated the concentrations and introduced a powerful push towards extended season, thus offsetting the early bias of the other models. Since median largely ignored this push, its performance was closer to that of other models. Nevertheless, both mean and median demonstrated low RMSE, median being marginally better.

5.2.2. Fusing the model predictions and observations into an optimized ensemble: gain in the analysis and predictive capacity

Developing further the ensemble technology, we present here the first attempt of fusion of the observational data with the multi-model ensemble for olive pollen.

In the Section 3.1, the Eq. (2) requires three parameters to prescribe: the regularization scaling parameters α and β , and length of the assimilation window T . For the purposes of the current feasibility study, several values for each of the parameters were tested and the robust performance of the ensemble was confirmed with very modest regularization strength and for all considered lengths of the analysis window – from 1 to 15 days. Finally, $\alpha=0.1$, $\beta=0.1$, $T=5\text{ days}$ were selected for the below example as a compromise between the smoothness of the coefficients, regularization strength and the optimization efficiency over the assimilation window.

813 The optimized ensemble showed (Figure 11, left-hand panel) that each of the 6 models had
814 substantial contribution over certain parts of the period. Over some times, e.g. during the first half
815 of May, only one or two models were used, other coefficients being put to zero, whereas closer to
816 the end of the month, all models were involved. Finally, prior to and after the main season,
817 concentrations were very low and noisy, so the regularization terms of Eq. (2) took over and pushed
818 the weights to a-priori value of 1/6.

819 The bulk of the improvements came in the first half of the season (Figure 11, middle panel). After
820 the third peak in the middle of May, the effect of assimilation becomes small and the optimization
821 tends to use intercept to meet the mean value, whereas the model predictions become small and
822 essentially uncorrelated with the observations. This corroborates with the observed 8-days shift of
823 the season, which fades out faster in the models than in the observed time series (Figure 10).

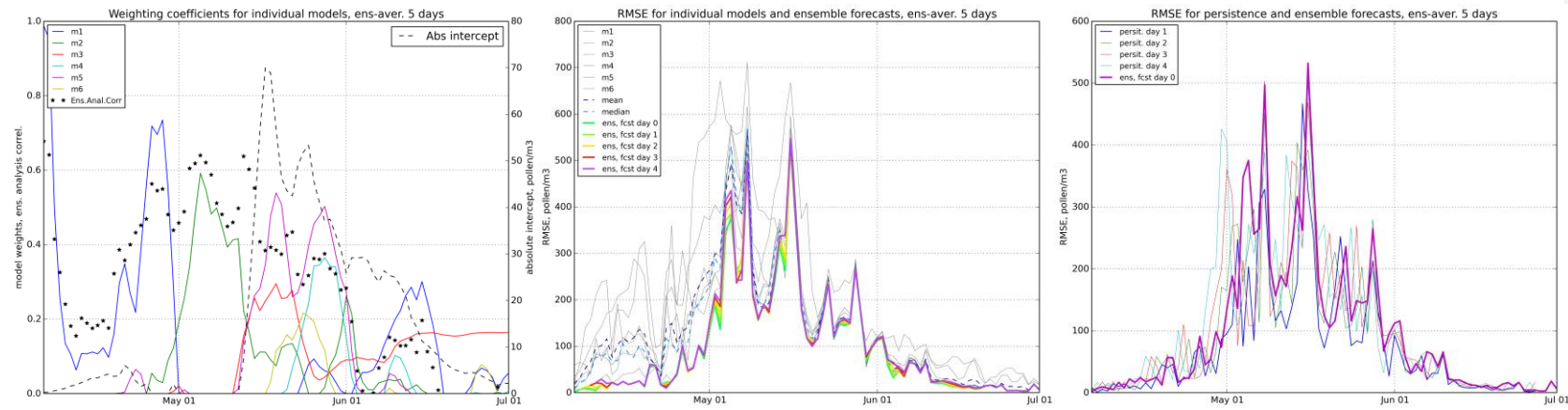
824 There was little reduction of the predictive capacity of the optimized ensemble when going out of
825 assimilation window towards the forecasts. In-essence, only the first peak of concentrations (and
826 RMSE) is better off with shorter forecasts. For the rest of the season (before and after the peak) the
827 5-day assimilation window led to a robust combination of the models that stayed nearly-optimal
828 over the next five days.

Deleted: 7

829 Comparison with other forecasts expectedly shows that the optimized ensemble not only has
830 significantly better skills than any of the individual models, but is up to 25-30% better than mean
831 and median of the ensemble (Figure 11, middle panel). A stronger competitor was the “persistence
832 forecast” when the next-day(s) concentrations are predicted to be equal the last observed daily
833 value. The one-day persistence appeared to be the best-possible “forecast”, which shows at the
834 beginning of May almost twice lower RMSE than the one-day forecast of the optimal ensemble
835 (Figure 11, right-hand panel). However, already two-days persistence forecast had about-same
836 RMSE as the ensemble, and 3- and 4- days predictions were poor.

Deleted: also

839



840

841

842

843

Figure 11. Optimal weights of the individual models and ensemble correlation score over the 5-days-long assimilation window (left panel); RMSE of the of individual models and the optimal ensemble forecasts against those of individual models and simple ensemble means (middle) and against persistence-based forecasts (right-hand panel).

844 Strong performance of the one-day persistence forecast is not surprising and, with the current
845 standards of the pollen observations, has no practical value: the data are always late by more than
846 one day (counting can start only next morning and become available about mid-day). The second
847 problem of the persistence forecast is that it needs actual data, i.e. the scarcity of pollen network
848 then limits its coverage. Thirdly, persistence loses its skills very fast: already day+2 forecast has no
849 superiority to the optimal ensemble, whereas day+3 and +4 persistence-based predictions are
850 useless. Finally, at local scale, state-of-art statistical models can outperform it – see discussion in
851 (Olga Ritenberga et al., 2016).

852 One should however point out that one-day predicting power of the persistence forecast (or more
853 sophisticated statistical models based on it) can be a strong argument for the future real-time online
854 pollen monitoring, which delay can be as short as one hour (Crouzy et al., 2016; Oteros et al.,
855 2015). Such data have good potential as the next-day predictions for the vicinity of the monitor.

856 5.3.Sensitivity of the simulations to model and source term parameters

857 The above-presented results show that arguably the most-significant uncertainty was due to shifting
858 the start and the end of the season. It originated from the long heat sum accumulation (since 1
859 January), where even a small systematic difference between the meteorology driving the multi-
860 annual fitting simulations and that used for operational forecasts integrates to a significant season
861 shift by late spring. In some areas, resolution of NWP model plays as well: complex terrain in the
862 north of Spain and in Italy requires dense grids to resolve the valleys. Other possible sources of
863 uncertainties might need attention.

864 To understand the importance of some key parameters, a series of perturbed runs of SILAM was
865 made:

- 866 - **os100** and **os150** runs with the season starting threshold increased by 100 and 150 degree
867 days (the **os150** run is referred in the above discussion as SILAMos150)
- 868 - **era** run with ERA-Interim meteorological fields, which were used for the source parameters
869 fitting
- 870 - series of 3 runs with reduced vertical mixing within the ABL and the free troposphere
- 871 - **smlpoll** run with 20 µm size of the pollen grain
- 872 - **smlpoll_coarse** run with 20 µm pollen size and coarse computational grid (0.2°×0.2°)

873

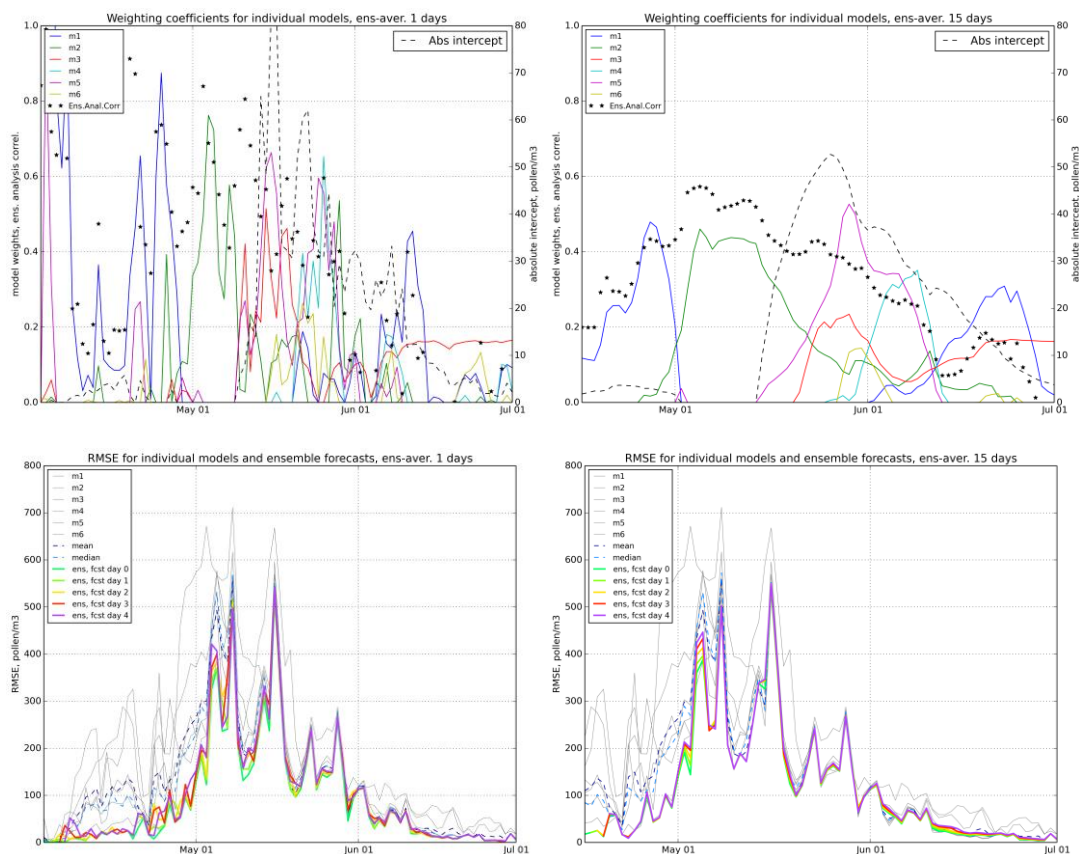


Figure 12. Sensitivity of optimized ensemble to the length of assimilation window. Upper row: optimal weights of the individual models and ensemble score over the 1- (left) and 15- (right) days-long assimilation windows; lower row: RMSE of the of individual models and the optimal ensemble forecasts against those of individual models. Obs. earlier first available date for 1-day-analysis window.

The **era** simulations with ERA-Interim reduced the shift of the season start by 2 days but increased the shift of the end by 3 days, i.e. made the season shorter by 5 days. At the same time, the **os150** run showed that a simple increase of the heat sum threshold by ~10% (150 degree days) essentially eliminates the mean shift – for 2014 – but it remains unclear whether this adjustment is valid for other years.

Variations of the mixing parameterization (perturbing the formula for the K_z eddy diffusivity) did not lead to significant changes: all scores stayed within 10% of the reference SILAM simulations.

887 Evaluation of the impact of deposition parameterizations was more difficult since they are model-
888 specific. Higher deposition intensity causes both reduction of the transport distance and absolute
889 concentrations. This issue might be behind the low values reported by LOTOS-EUROS and,
890 conversely, high concentrations of EURAD-IM and MOCAGE. Its importance was confirmed by
891 the SILAM sensitivity simulations with smaller pollen size, **smlpoll** and **smlpoll_coarse**. Both runs
892 resulted in more than doubling the mean concentrations but with marginal effect on temporal
893 correlation. They also differed little from each other.

894 Variations of the fusion parameters showed certain effect. For short averaging window (5 days or
895 less), the variations of weighting coefficients increased and the time series became noisier (Figure
896 12). On return, the correlation increased almost up to 0.8 – 0.9 for some analysis intervals, though
897 stayed the same for other periods. Also, the one-day forecast RMSE decreased for some days but
898 little difference was found for longer predictions.

5.4. Main challenges for the future

The current study is the first application of numerical models to olive pollen dispersion in Europe.

One of its objectives was to identify the most-pressing limitations of the current approach and the extent to which the ensemble and data fusion technologies can help in improving the forecasts.

The most-evident issue highlighted by the exercise is the shift of the pollen season, which is similar in all models suggesting some unresolved inconsistencies between the heat-sum calculations of the source term and the features of the temperature predictions by the weather model. The issue suggests some factor(s) currently not included or mis-interpreted in the source term. One of the candidate processes is the chilling-sum accumulation suggested by some studies, e.g., (Aguilera et al., 2014). A switch to different types of phenological models with genetic differentiation of the populations following Chuine and Belmonte, (2004) is another promising option.

The second issue refers to the under-estimation of the pollen concentration in France, which probably originates from a comparatively large number of olive trees spread in private gardens etc but not accounted for in the agriculture maps of olive plantations.

The third set of questions refers to the pollen load prediction, i.e. a possibility to forecast the overall season severity before it starts. Several statistical models have been presented in the literature, e.g., (Ben Dhiab et al., 2016) for total annual load and (Chuine and Belmonte, 2004) for relative load. Their evaluation and implementation in the context of dispersion models is important.

Deleted: ¶

Formatted: Heading 2

Deleted: and o

Deleted: ,

Deleted: the

Deleted: ing presence of

Deleted: (

Deleted: distributed

924 An issue, mostly addressing the long-term horizon rather than the short-term forecasts is the validity
925 of the developed models in the conditions of changing climate. The models have to be robust to the
926 trends in meteorological forcing. Purely statistical models are among the most vulnerable in this
927 respect because they just quantify the apparent correlations observed under certain conditions but
928 do not explore the processes behind these relations.

Deleted: important

Deleted: , ???????????????

929 Finally, already the first steps towards ensemble-based fusion of the model forecasts and pollen
930 observations showed strong positive effect. Further development of these techniques combined with
931 progress towards near-real-time pollen data has very high potential for improving the forecasts.

Deleted: ve

Deleted: effect on

Deleted: quality

933 6. Summary

934 An ensemble of 6 CAMS models was run through the olive flowering season of 2014 and compared
935 with observational data of 6 countries of European Aeroallergen Network (EAN).

936 The simulations showed decent level of reproduction of the short-term phenomena but also
937 demonstrated a shift of the whole season by 8 days (~20% of the overall pollination period). An ad-
938 hoc adjustment of the season-start heat sum threshold by ~10% (150 degree days) resolves the issue
939 and strongly improves the model skills but its validity for other years and meteorological drivers
940 remain unclear.

941 The ensemble members showed quite diverse pictures demonstrating the substantial variability,
942 especially in areas remote from the main olive plantations. Nevertheless, the observation rank
943 histogram still suggested certain under-statement of the ensemble variability in comparison with the
944 observations. This partly originates from the synchronized source term formulations and
945 meteorological input used by all but one models.

Deleted: same

946 Simple ensemble treatments, such as arithmetic average and median, resulted in a more robust
947 performance but they did not outrun the best models over significant parts of the season. Arithmetic
948 average turned out to be better than median.

949 A data-fusion approach, which creates the optimal-ensemble model using the observations over
950 preceding days for optimal combination of the ensemble members, is suggested and evaluated. It
951 was based on an optimal linear combination of the individual ensemble members and showed strong
952 skills, routinely outperforming all individual models and simple ensemble approaches. It also
953 showed strong forecasting skills, which allowed application of the past-time model weighting

960 coefficients over several days in the future. The only approach outperforming this fusion ensemble
961 was the one-day persistence-based forecast, which has no practical value due to the manual pollen
962 observations and limited network density. It can however be used in the future when reliable online
963 pollen observation will become available.

964 A series of sensitivity simulations highlighted the importance of meteorological driver, especially
965 its temperature representation, and deposition mechanisms. The data fusion procedure was quite
966 robust with regard to analysis interval, still requiring 5-7 days for eliminating the noise in the model
967 weighting coefficients.

968

969 7. Acknowledgements

970 The work was performed within the scope of Copernicus Atmospheric Monitoring Service CAMS,
971 funded by the European Union's Copernicus Programme. Support by performance-based funding of
972 University of Latvia is also acknowledged. Observational data were provided by national pollen
973 monitoring of Croatia, Greece, France, Italy ([A.I.A.-R.I.M.A.[®]](#)), Spain ([REA: Aerocam, AeroUEx,](#)
974 [RAA, UO, UC and Cantabria Health Council, REDAEROCAM, Health Castilla-Leon Council,](#)
975 [RACyL, XAC, RIAG, PalinoCAM, UPCT, Basque Government / Public Health Directory](#)), Turkey,
976 members of the European Aeroallergen Network EAN. The olive source term is a joint
977 development of Finnish Meteorological Institute and EAN research teams, created within the scope
978 of the Academy of Finland APTA project. This work contributes to the ICTA 'Unit of Excellence'
979 (MinECo, MDM2015-0552).

980 The material is published in the name of the European Commission; the Commission is not
981 responsible for any use that may be made of the information/material contained.

982

983 8. References

- 984 Aguilera, F., Ben Dhiab, A., Msallem, M., Orlandi, F., Bonofiglio, T., Ruiz-Valenzuela, L., Galán,
985 C., Díaz-de la Guardia, C., Giannelli, A., Trigo, M.M., García-Mozo, H., Pérez-, Badia, R.,
986 Fornaciari, M., 2015. Airborne-pollen maps for olive-growing areas throughout the
987 Mediterranean region: spatio-temporal interpretation. *Aerobiologia* (Bologna). 31, 421–434.
- 988 Aguilera, F., Fornaciari, M., Ruiz-Valenzuela, L., Galán, C., Msallem, M., Dhiab, A. Ben, la
989 Guardia, C.D. de, del Mar Trigo, M., Bonofiglio, T., Orlandi, F., 2014. Phenological models to
990 predict the main flowering phases of olive (*Olea europaea* L.) along a latitudinal and

Formatted: Not Highlight

991 longitudinal gradient across the Mediterranean region. *Int. J. Biometeorol.* 59, 629–641.
992 doi:10.1007/s00484-014-0876-7

993 Aguilera, F., Ruiz, L., Fornaciari, M., Romano, B., Galán, C., Oteros, J., Ben Dhiab, A., Msallem,
994 M., Orlandi, F., 2013. Heat accumulation period in the Mediterranean region: phenological
995 response of the olive in different climate areas (Spain, Italy and Tunisia). *Int. J. Biometeorol.*
996 58, 867–876.

997 Alba, F., Di?az De La Guardia, C., 1998. The effect of air temperature on the starting dates of the
998 Ulmus, Platanus and Olea pollen seasons in the SE Iberian Peninsula. *Aerobiologia (Bologna)*.
999 14, 191–194.

1000 Andersen, T.B., 1991. A model to predict the beginning of the pollen season. *Grana* 30, 269–275.
1001 doi:10.1080/00173139109427810

1002 Baklanov, A., Sorensen, J.H., 2001. Parameterisation of radionuclide deposition in atmospheric
1003 long-range transport modelling. *Phys. Chem. Earth, Parts B* 26, 787–799.

1004 Barranco, D., Fernández-Escobar, R., Rallo, L., 2008. *El Cultivo del olivo* (8^a Ed). Madrid.

1005 Bechtold, P., Bazile, E., Guichard, F., Mascart, P., Richard, E., 2001. A mass-flux convection
1006 scheme for regional and global models. *Quarterly J. R. Meteorol. Soc.* 127, 869–886.

1007 Ben Dhiab, A., Ben Mimoun, M., Oteros, J., Garcia-Mozo, H., Domínguez-Vilches, E., Galán, C.,
1008 Abichou, M., Msallem, M., 2016. Modeling olive-crop forecasting in Tunisia. *Theor. Appl.*
1009 *Climatol.* 1–9. doi:10.1007/s00704-015-1726-1

1010 Bott, A., 1989. A positive definite advection scheme obtained by nonlinear renormalization of the
1011 advective fluxes. *Mon. Weather Rev.* 117, 1006–1016.

1012 Buters, J., Prank, M., Sofiev, M., Pusch, G., Ing, D., Berger, U., Brandao, R., Celenk, S., Galan, C.,
1013 Reese, G., Sauliene, I., Jackowiak, B., Kennedy, R., Rantio-lehtim, A., Smith, M., Thibaudon,
1014 M., Weber, B., Cecchi, L., 2015. Variation of the group 5 grass pollen allergen content of
1015 airborne pollen in relation to geographic location and time in season. *J. Allergy Clin. Immunol.*
1016 136, 87–95. doi:10.1016/j.jaci.2015.01.049

1017 Buters, J.T.M., Thibaudon, M., Smith, M., Kennedy, R., Rantio-Lehtim?ki, A., Albertini, R., Reese,
1018 G., Weber, B., Galan, C., Brandao, R., Antunes, C.M., J?ger, S., Berger, U., Celenk, S.,
1019 Grewling, T., Jackowiak, B., Sauliene, I., Weichenmeier, I., Pusch, G., Sarioglu, H., Ueffing,
1020 M., Behrendt, H., Prank, M., Sofiev, M., Cecchi, L., 2012. Release of Bet v 1 from birch
1021 pollen from 5 European countries. Results from the HIALINE study. *Atmos. Environ.* 55.
1022 doi:10.1016/j.atmosenv.2012.01.054

1023 Cebrino, J., Portero de la Cruz, S., Barasona, M.J., Alcázar, P., Moreno, C., Domínguez-Vilches, E.,
1024 Galán, C., 2017. Airborne pollen in Córdoba City (Spain) and its implications for pollen
1025 allergy. *Aerobiologia (Bologna)*. 33, 281–291. doi:10.1007/s10453-016-9469-8

1026 CEC, 1993. *CORINE Land Cover Technical Guide*. Luxembourg.

1027 Champeaux, J.L., Masson, V., Chauvin, F., 2005. ECOCLIMAP: a global database of land surface
1028 parameters at 1 km resolution. *Meteorol. Appl.* 29–32.

1029 Chuine, I., Belmonte, J., 2004. Improving prophylaxis for pollen allergies : Predicting the time
1030 course of the pollen load of the atmosphere of major allergenic plants in France and Spain.
1031 *Grana* 43, 65–80. doi:10.1080/00173130410019163

1032 Crouzy, B., Stella, M., Konzelmann, T., Calpini, B., Clot, B., 2016. All-optical automatic pollen
1033 identification: Towards an operational system. *Atmos. Environ.* 140, 202–212.

doi:10.1016/j.atmosenv.2016.05.062

D'Amato, G., Cecchi, L., Bonini, S., Nunes, C., Annesi-Maesano, I., Behrendt, H., Liccardi, G., Popov, T., van Cauwenberge, P., 2007. Allergenic pollen and pollen allergy in Europe. *Allergy* 62, 976–990. doi:10.1111/j.1398-9995.2007.01393.x

D'Amato, G., Cecchi, L., Bonini, S., Nunes, C., Annesi-Maesano, I., Behrendt, H., Liccardi, G., Popov, T., van Cauwenberge, P., 2007. Allergenic pollen and pollen allergy in Europe. *Allergy* 62, 976–990.

de Weger, L., Bergmann, K.-C., Rantio-Lehtimäki, A., Dahl, Å., Buters, J.T.M., Dechamp, C., Belmonte, J., Thibaudon, M., Cecchi, L., Besancenot, J.-P., Gala, C., Waisel, Y., 2013. Impact of pollen, in: Sofiev, M., Bergmann, K.-C. (Eds.), *Allergenic Pollen. A Review of the Production, Release, Distribution and Health Impacts*. Springer Netherlands, Dordrecht, p. x + 247. doi:10.1007/978-94007-4881-1

Elbern, H., Strunk, A., Schmidt, H., Talagrand, O., 2007. Emission rate and chemical state estimation by 4-dimensional variational inversion. *Atmos. Chem. Phys.* 7, 3749–3769.

Fernandez-Escobar, R., Benlloch, M., Navarro, C., G.C., M., 1992. The Time of Floral Induction in the Olive. *J. Am. Soc. Hortic. Sci.* 117, 304–307.

Fornaciari, M., Pieroni, L., Ciuchi, P., Romano, B., 1998. A regression model for the start of the pollen season in *Olea europaea*. *Grana* 37, 110–113.

Frenguelli, G., Bricchi, E., Romano, B., Mincigrucci, G., Spieksma, F.T.M., 1979. A predictive study on the beginning of the pollen season for Gramineae and *Olea europaea* L. *Aerobiologia* (Bologna). 5, 64–70.

Gala, C., Garcia-Mozo, H., Carinanos, P., Alcazar, P., Dominguez-Vilches, E., 2001. The role of temperature in the onset of the *Olea europaea* L. pollen season in southwestern Spain. *Int. J. Biometeorol.* 45, 8–12.

Galan, C., Alcazar, P., Oteros, J., Garcia-Mozo, H., Aira, M.J., Belmonte, J., Diaz de la Guardia, C., Fernandez-Gonzalez, D., Gutierrez-Bustillo, M., Moreno-Grau, S., Perez-Badia, R., Rodriguez-Rajo, J., Ruiz-Valenzuela, L., Tormo, R., Trigo, M.M., Dominguez-Vilches, E., 2016. Airborne pollen trends in the Iberian Peninsula. *Sci. Total Environ.* 550, 53–59. doi:10.1016/j.scitotenv.2016.01.069

Galan, C., Antunes, C., Brandao, R., Torres, C., Garcia-Mozo, H., Caeiro, E., Ferro, R., Prank, M., Sofiev, M., Albertini, R., Berger, U., Cecchi, L., Celenk, S., Grewling, L., Jackowiak, B., Jäger, S., Kennedy, R., Rantio-Lehtimäki, A., Reese, G., Sauliene, I., Smith, M., Thibaudon, M., Weber, B., Weichenmeier, I., Pusch, G., Buters, J.T.M., 2013. Airborne olive pollen counts are not representative of exposure to the major olive allergen *Olea* 1. *Allergy Eur. J. Allergy Clin. Immunol.* 68. doi:10.1111/all.12144

Galán, C., García-Mozo, H., Vázquez, L., Ruiz, L., De La Guardia, C.D., Trigo, M., 2005. Heat requirement for the onset of the *Olea europaea* L. pollen season in several sites in Andalusia and the effect of the expected future climate change. *Int. J. Biometeorol.* 49, 184–188.

Galán, C., Smith, M., Thibaudon, M., Frenguelli, G., Oteros, J., Gehrig, R., Berger, U., Clot, B., Brandao, R., Group, E.Q.W., 2014. Pollen monitoring: minimum requirements and reproducibility of analysis. *Aerobiologia* (Bologna). 30, 385–395.

García-mozo, H., Galán, C., Jato, V., Belmonte, J., Díaz, C., Guardia, D., Fernández, D., Aira, M.J., Roure, J.M., Ruiz, L., Trigo, M.M., Domínguez-vilches, E., 2006. *Quercus* pollen season dynamics in the Iberian Peninsula: response to meteorological parameters and possible

consequences of climate change. *Ann. Agric. Environ. Med.* 209–224.

Garcia-Mozo, H., Yaezel, L., Oteros, J., Galan, C., 2014. Statistical approach to the analysis of olive long-term pollen season trends in southern Spain. *Sci. Total Environ.* 473–474, 103–109. doi:10.1016/j.scitotenv.2013.11.142

Genikhovich, E., Pavlova, T. V., Kattsov, V.M., 2010. On complexing the ensemble of climate models (In Russian: O kompleksirovanii ansamblya klimaticheskikh modelej). *Proc. Voeikov Main Geophysical Obs.* 7, 28–46.

Giorgi, F., Chameides, W.L., 1986. Rainout lifetimes of highly soluble aerosols and gases as inferred from simulations with a general circulation model. *J. Geophys. Res.* 91, 14367–14376.

Gioulekas, D., Papakosta, D., Damialis, A., Spieksma, F.T.M., Giouleka, P., Patakas, D., 2004. Allergenic pollen records (15 years) and sensitization in patients with respiratory allergy in Thessaloniki , Greece. *Allergy* 174–184.

Gómez, J.A., Infante-Amate, J., González de Molina, M., Vanwalleghem, T., Taguas, E.V., Lorite, I., 2014. Olive Cultivation, its Impact on Soil Erosion and its Progression into Yield Impacts in Southern Spain in the Past as a Key to a Future of Increasing Climate Uncertainty. *Agriculture* 4, 170–198. doi:10.3390/agriculture4020170

Hass, H., Jakobs, H.J., Memmesheimer, M., 1995. Analysis of a regional model (EURAD) near surface gas concentration predictions using observations from networks. *Meteorol. Atmos. Phys.* 57, 173–200.

Hirst, J.M., 1952. An automatic volumetric spore trap. *Ann. Appl. Biol.* 39, 257–265. doi:10.1111/j.1744-7348.1952.tb00904.x

Holtslag, A.A., Nieuwstadt, F.T.M., 1986. Scaling the atmospheric boundary layer. *Bound. Layer Meteorol.* 36, 201–209.

Johansson, L., Epitropou, V., Karatzas, K., Karppinen, A., Wanner, L., Vrochidis, S., Bassoukos, A., Kukkonen, J., Kompatsiaris, I., 2015. Fusion of meteorological and air quality data extracted from the web for personalized environmental information services. *Environ. Model. Softw.* 64, 143–155. doi:10.1016/j.envsoft.2014.11.021

Josse, B., Simon, P., Peuch, V., 2004. Radon global simulations with the multiscale chemistry and transport model MOCAGE. *Tellus B* 56, 339–356.

Jäger, S., Mandroli, P., Spieksma, F., Emberlin, J., Hjelmroos, M., Rantio-Lehtimäki, A., Al, E., 1995. *News. Aerobiologia (Bologna)*. 11, 69–70.

Kalyoncu, A., Qoplii, L., Selguk, Z., Emri, A., Kolagan, B., Kocabas, A., 1995. Survey of the allergic status of patients with bronchial asthma in Turkey : a multicenter study. *Allergy* 50, 451–456.

Kouznetsov, R., Sofiev, M., 2012. A methodology for evaluation of vertical dispersion and dry deposition of atmospheric aerosols. *J. Geophys. Res.* 117. doi:doi:10.1029/2011JD016366

Kukkonen, J., Olsson, T., Schultz, D.M., Baklanov, a., Klein, T., Miranda, a. I., Monteiro, a., Hirtl, M., Tarvainen, V., Boy, M., Peuch, V.-H., Poupkou, a., Kioutsioukis, I., Finardi, S., Sofiev, M., Sokhi, R., Lehtinen, K.E.J., Karatzas, K., San José, R., Astitha, M., Kallos, G., Schaap, M., Reimer, E., Jakobs, H., Eben, K., 2012. A review of operational, regional-scale, chemical weather forecasting models in Europe. *Atmos. Chem. Phys.* 12, 1–87. doi:10.5194/acp-12-1-2012

Langner, J., Bergström, R., Pleijel, K., 1998. European scale modeling of sulphur, oxidized nitrogen

and photochemical oxidants. Model dependent development and evaluation for the 1994 growing season. Norkoping.

Linkosalo, T., Ranta, H., Oksanen, A., Siljamo, P., Luomajoki, A., Kukkonen, J., Sofiev, M., 2010. A double-threshold temperature sum model for predicting the flowering duration and relative intensity of *Betula pendula* and *B. pubescens*. *Agric. For. Meteorol.* 6–11. doi:10.1016/j.agrformet.2010.08.007

Louis, J.-F., 1979. A parametric model of vertical eddy fluxes in the atmosphere. *Bound. Layer Meteorol.* 17, 187–202.

Loureiro, G., Rabaca, M.A., Blanco, B., Andrade, S., Chieira, C., Pereira, C., 2005. Aeroallergens' sensitization in an allergic paediatric population of Cova da Beira, Portugal. *Allergol. Immunopathol. (Madr)*. 33, 192–198.

Mandrioli, P., Comtois, P., V., L. (Eds.), 1998. *Methods in Aerobiology*. Pitagora Editrice, Bologna.

Marécal, V., Peuch, V.-H., Andersson, C., Andersson, S., Arteta, J., Beekmann, M., Benedictow, A., Bergström, R., Bessagnet, B., Cansado, A., Chéroux, F., Colette, A., Coman, A., Curier, R.L., Denier van der Gon, H. a. C., Drouin, A., Elbern, H., Emili, E., Engelen, R.J., Eskes, H.J., Foret, G., Friese, E., Gauss, M., Giannaros, C., Guth, J., Joly, M., Jaumouillé, E., Josse, B., Kadygrov, N., Kaiser, J.W., Krajsek, K., Kuenen, J., Kumar, U., Liora, N., Lopez, E., Malherbe, L., Martinez, I., Melas, D., Meleux, F., Menut, L., Moinat, P., Morales, T., Parmentier, J., Piacentini, A., Plu, M., Poupkou, A., Queguiner, S., Robertson, L., Rouil, L., Schaap, M., Segers, A., Sofiev, M., Thomas, M., Timmermans, R., Valdebenito, Á., van Velthoven, P., van Versendaal, R., Vira, J., Ung, A., 2015. A regional air quality forecasting system over Europe: the MACC-II daily ensemble production. *Geosci. Model Dev.* 8, 2777–2813. doi:10.5194/gmd-8-2777-2015

Martet, M., Peuch, V.-H., Laurent, B., B., M., Bergametti, G., 2009. Evaluation of long-range transport and deposition of desert dust with the CTM Mocage. *Tellus B* 61, 449–463.

Masson, V., Champelaur, J.-L., Chauvin, F., Meriguet, C., Lacaze, R., 2003. A Global Database of Land Surface Parameters at 1-km Resolution in Meteorological and Climate Models. *J. Clim.* 16, 1261–1282.

Memmesheimer, M., Friese, E., Ebel, A., Jakobs, H.J., Feldmann, H., Kessler, C., Piekorz, G., 2004. Long-term simulations of particulate matter in Europe on different scales using sequential nesting of a regional model. *Int. J. Environ. Pollut.* 22, 108–132.

Moriondo, M., Orlandini, S. De, P., N., Mandrioli, P., 2001. Effect of agrometeorological parameters on the phenology of pollen emission and production of olive trees (*Olea europaea* L.). *Aerobiologia (Bologna)*. 225–232. doi:doi:10.1023/A:1011893411266

Negrini, A.C., Ariano, R., Delbono, G., Ebbli, A., Quaglia, A., Arobba, D., Allergologia, A., Paolo, O.S., Ligure, P., Sv, I.-P.L., 1992. Incidence of sensitisation to the pollens of *Urticaceae* (*Parietaria*), *Poaceae* and *Oleaceae* (*Olea europaea*) and pollen rain in Liguria (Italy). *Aerobiologia (Bologna)*. 8, 355–358.

Orlandi, F., Lanari, D., Romano, B., Fornaciari, M., 2006. New model to predict the timing of olive (*Olea europaea*) flowering: a case study in central Italy. *New Zeal. J. Crop Hortic. Sci.* 34, 93–99. doi:10.1080/01140671.2006.9514392

Orlandi, F., Romano, B., Fornaciari, M., 2005a. Effective pollination period estimation in olive (*Olea europaea* L.): A pollen monitoring application. *Sci. Hortic. (Amsterdam)*. 313–318.

doi:doi:10.1016/j.scienta.2005.01.012

Orlandi, F., Vazquez, L.M., Ruga, L., Bonofiglio, T., Fornaciari, M., Garcia-Mozo, H., Domínguez, E., Romano, B., Galan, C., 2005b. Bioclimatic requirements for olive flowering in two mediterranean regions located at the same latitude (Andalucia, Spain, and Sicily, Italy). *Ann. Agric. Environ. Med.* 47–52.

Oteros, J., Garcia-Mozo, H., Vazquez, L., Mestre, A., Dominguez-Vilches, E., Galan, C., 2013. Modelling olive phenological response to weather and topography. *Agric. Ecosyst. Environ.* 179, 62–68.

Oteros, J., García-Mozo, H., Alcázar, P., Belmonte, J., Bermejo, D., Boi, M., Cariñanos, P., Díaz de la Guardia, C., Fernández-González, D., González-Minero, F., Gutiérrez-Bustillo, A.M., Moreno-Grau, S., Pérez-Badia, R., Rodríguez-Rajo, F.J., Ruíz-Valenzuela, L., Suárez-Pérez, J., Trigo, M.M., Domínguez-Vilches, E., Galán, C., 2015. A new method for determining the sources of airborne particles. *J. Environ. Manage.* 155, 212–218.

Oteros, J., Orlandi, F., Aguilera, F., Ben, A., Bonofiglio, T., 2014. Better prediction of Mediterranean olive production using pollen-based models. *Agron. Sustain. Dev.* 34, 685–694. doi:10.1007/s13593-013-0198-x

Oteros, J., Pusch, G., Weichenmeier, I., Heimann, U., Möller, R., Röseler, S., Traidl-Hoffmann, C., Schmidt-Weber, C., Buters, J.T.M., 2015. Automatic and online pollen monitoring. *Int. Arch. Allergy Immunol.* 167, 158–166. doi:10.1159/000436968

Pereira, C., Valero, A., Loureiro, C., Dávila, I., 2006. IBERIAN STUDY OF AEROALLERGENS SENSITISATION IN ALLERGIC RHINITIS. *Eur. Ann. Allergy Clin. Immunol.* 38, 186–194.

Petroff, A., Zhang, L., 2010. Development and application of a size-resolved particle dry deposition scheme for application in aerosol transport models. *Geosci. Model Dev.* 3, 753–769. doi:doi:10.5197/gmd-3-753-2010

Potempski, S., Galmarini, S., 2009. and Physics Est modus in rebus : analytical properties of multi-model ensembles. *Atmos. Chem. Phys.* 9, 9471–9489.

Prank, M., Chapman, D.S., Bullock, J.M., Belmonte, J., Berger, U., Dahl, A., Jäger, S., Kovtunen, I., Magyar, D., Niemelä, S., Rantio-Lehtimäki, A., Rodinkova, V., Sauliene, I., Severova, E., Sikoparija, B., Sofiev, M., 2013. An operational model for forecasting ragweed pollen release and dispersion in Europe. *Agric. For. Meteorol.* 182–183, 43–53. doi:10.1016/j.agrformet.2013.08.003

Ritenberga, O., Sofiev, M., Kirillova, V., Kalnina, L., Genikhovich, E., 2016. Statistical modelling of non-stationary processes of atmospheric pollution from natural sources : example of birch pollen. *Agric. For. Meteorol.* 226–227, 96–107. doi:10.1016/j.agrformet.2016.05.016

Ritenberga, O., Sofiev, M., Kirillova, V., Kalnina, L., Genikhovich, E., 2016. Statistical modelling of non-stationary processes of atmospheric pollution from natural sources: Example of birch pollen. *Agric. For. Meteorol.* 226–227. doi:10.1016/j.agrformet.2016.05.016

Robertson, L., Langner, J., 1999. An Eulerian Limited-Area Atmospheric Transport Model. *J. Appl. Meteorol.* 38, 190–210.

Rojo, J., Orlandi, F., Perez-Badia, R., Aguilera, F., Ben Dhiab, A., Bouziane, H., Diaz de la Guardia, C., Galan, C., Gutierrez-Bustillo, A.M., Moreno-Grau, S., Msallem, M., Trigo, M.M., Fornaciari, M., 2016. Modeling olive pollen intensity in the Mediterranean region through analysis of emission sources. *Sci. Total Environ.* 551–552, 73–82. doi:10.1016/j.scitotenv.2016.01.193

1209 Rojo, J., Pérez-Badia, R., 2015. Spatiotemporal analysis of olive flowering using geostatistical
1210 techniques. *Sci. Total Environ.* 505, 860–869.

1211 Sánchez-Mesa, J.A., Serrano, P., Cariñanos, P., Prieto-Baena, J., Moreno, C., Guerra, F., Galan, C.,
1212 2005. Pollen allergy in Cordoba city: frequency of sensitization and relation with antihistamine
1213 sales. *J. Investig. Allergol. Clin. Immunol.* 15, 50–56.

1214 Schaap, M., Timmermans, R. M. A., Roemer, M., Boersen, G.A.C., Builtjes, P.J.H., Sauter, F.J.,
1215 Velders, G.J.M., Beck, J.P., 2008. The LOTOS-EUROS model: Description, validation and
1216 latest developments. *Int. J. Environ. Pollut.* 32, 270–290.

1217 Scott, B.C., 1979. Parameterization of sulphate removal by precipitation. *J. Appl. Meteorol.* 17,
1218 11275–11389.

1219 Seinfeld, J.H., Pandis, S.N., 1998. *Atmospheric Chemistry and Physics*, 1st ed. Wiley, New York.

1220 Siljamo, P., Sofiev, M., Ranta, H., Linkosalo, T., Kubin, E., Ahas, R., Genikhovich, E., Jatczak, K.,
1221 Jato, V., Nekovar, J., Minin, A., Severova, E., Shalabova, V., 2008. Representativeness of
1222 point-wise phenological *Betula* data collected in different parts of Europe. *Glob. Ecol.*
1223 *Biogeogr.* 17, 489–502. doi:10.1111/j.1466-8238.2008.00383.x

1224 Simpson, D., Benedictow, a., Berge, H., Bergström, R., Emberson, L.D., Fagerli, H., Flechard,
1225 C.R., Hayman, G.D., Gauss, M., Jonson, J.E., Jenkin, M.E., Nyíri, a., Richter, C., Semeena,
1226 V.S., Tsyro, S., Tuovinen, J.-P., Valdebenito, Á., Wind, P., 2012. The EMEP MSC-W
1227 chemical transport model – technical description. *Atmos. Chem. Phys.* 12, 7825–7865.
1228 doi:10.5194/acp-12-7825-2012

1229 Simpson, D., Fagerli, H., Jonson, J.E., Tsyro, S., Wind, P., Tuovinen, J.-P., 2003. Transboundary
1230 Acidification, Eutrophication and Ground Level Ozone in Europe, Part 1: Unified EMEP
1231 Model Description. EMEP Report 1/2003. Oslo.

1232 Sofiev, M., 2016. On impact of transport conditions on variability of the seasonal pollen index.
1233 *Aerobiologia* (Bologna). doi:10.1007/s10453-016-9459-x

1234 Sofiev, M., 2002. Extended resistance analogy for construction of the vertical diffusion scheme for
1235 dispersion models. *J. Geophys. Res.* 107, ACH 10-1–ACH 10-8. doi:10.1029/2001JD001233

1236 Sofiev, M., Berger, U., Prank, M., Vira, J., Arteta, J., Belmonte, J., Bergmann, K.C., Charoux, F.,
1237 Elbern, H., Friese, E., Galan, C., Gehrig, R., Khvorostyanov, D., Kranenburg, R., Kumar, U.,
1238 Marecal, V., Meleux, F., Menut, L., Pessi, A.-M., Robertson, L., Ritenberga, O., Rodinkova,
1239 V., Saarto, A., Segers, A., Severova, E., Sauliene, I., Siljamo, P., Steensen, B.M., Teinmaa,
1240 E., Thibaudon, M., Peuch, V.-H., 2015. MACC regional multi-model ensemble simulations of
1241 birch pollen dispersion in Europe. *Atmos. Chem. Phys.* 15, 8115–8130. doi:10.5194/acp-15-
1242 8115-2015

1243 Sofiev, M., Siljamo, P., Ranta, H., Linkosalo, T., Jaeger, S., Rasmussen, A., Rantio-Lehtimäki, A.,
1244 Severova, E., Kukkonen, J., 2012. A numerical model of birch pollen emission and dispersion
1245 in the atmosphere. Description of the emission module. *Int. J. Biometeorol.* 57, 54–58.
1246 doi:10.1007/s00484-012-0532-z

1247 Sofiev, M., Siljamo, P., Valkama, I., Ilvonen, M., Kukkonen, J., 2006. A dispersion modelling
1248 system SILAM and its evaluation against ETEX data. *Atmos. Environ.* 40, 674–685.
1249 doi:10.1016/j.atmosenv.2005.09.069

1250 Sofiev, M., Vira, J., Kouznetsov, R., Prank, M., Soares, J., Genikhovich, E., 2015. Construction of
1251 the SILAM Eulerian atmospheric dispersion model based on the advection algorithm of
1252 Michael Galperin. *Geosci. Model Dev.* 8. doi:10.5194/gmd-8-3497-2015

1253 Spano, D., Cesaraccio, C., Duce, P., Snyder, R.L., 1999. Phenological stages of natural species and
1254 their use as climate indicators. *Int. J. Biometeorol.* 124–133. doi:doi:10.1007/s004840050095

1255 Spielsma, F.T., 1990. Pollinosis in Europe: New observations and developments. *Rev. Palaeobot.*
1256 *Palynol.* 64, 35–40.

1257 Udvardy, O., Tedeschini, E., Sofiev, M., Palamarchuk, J., Makra, L., Kajtor-Apatini, D., Magyar,
1258 D., 2017. Utazo Allergenek Mediterran eredetu viragpor Magyarorszagon (in Hungarian).
1259 *Allergologia* June, 25–27.

1260 Venkatram, A., 1978. Estimating the convective velocity scale for diffusion applications. *Bound.*
1261 *Layer Meteorol.* 15, 447–452.

1262 Walcek, C.J., Aleksic, N.M., 1998. A simple but accurate mass conservative, peak-preserving,
1263 mixing ratio bounded advection algorithm with FORTRAN code. *Atmos. Environ.* 32, 3863–
1264 3880. doi:10.1016/S1352-2310(98)00099-5

1265 Williamson, D.L., Rasch, P., 1989. Two-Dimensional Semi-Lagrangian Transport with Shape-
1266 Preserving Interpolation. *Am. Meteorol. Soc.* 117, 102–129.

1267 Zhang, L., Gong, S., Padro, J., Barrie, L., 2001. A size-segregated particle dry deposition scheme
1268 for an atmospheric aerosol module. *Atmos. Environ.* 35, 549–560.

1269

1270